Design and Implementation of a Biomimetic Robotic Fish

Hongan Wang

A Thesis

in

The Department

of

Mechanical and Industrial Engineering

Presented in Partial Fulfillment of the Requirements

for the Degree of Master of Applied Science (Mechanical Engineering) at

Concordia University

Montreal, Quebec, Canada

October 2009

Your file Votre référence
ISBN: 978-0-494-67205-1
Our file Notre référence
ISBN: 978-0-494-67205-1

ABSTRACT

Design and Implementation of a Biomimetic Robotic Fish

Hongan Wang

The study of biomimetic robotic fish has received a growing amount of research interest in the past several years. This thesis describes the development and testing of a novel mechanical design of a biomimetic robotic fish. The robotic fish has a structure which uses oscillating caudal fins and a pair of pectoral fins to generate fish-like swimming motion. This unique design enables the robotic fish to swim in two swimming modes, namely Body/Caudal Fin (BCF) and Median/Paired Fin (MPF). In order to combine BCF mode with MPF mode, the robotic fish utilizes a flexible posterior body, an oscillating foil actuated by three servomotors, and one pair of pectoral fins individually driven by four servomotors. Effective servo motions and swimming gaits are then proposed to control its swimming behaviour. Based on these results, fish-like swimming can be achieved including forward, backward, and turning motions. An experimental setup for the robotic fish was implemented using machine vision position and velocity measurement. The experimental results show that the robotic fish performed well in terms of manoeuvrability and cruise speed. Based on the experimental data, a low order dynamic model is proposed and identified. Together, these results provide an experimental framework for development of new modelling and control techniques for biomimetic robotic fish.

Acknowledgments

This thesis was carried out in the Control and Information System Laboratory (CIS) at Concordia University, Montreal, Canada. I am grateful for having had the opportunity to be a part of the CIS research team.

I would like to thank my supervisor, Dr. Brandon Gordon, who not only helped me from a practical perspective, by showing me the way whenever I was lost and giving me ideas that were the key to solving my problems, but also taught me the philosophy of science and control engineering. A supervisor who possesses an understanding of both the science and its philosophy and who supports his students throughout all the ups and downs of their student life is rare to find and I am really happy (and lucky) that I had this opportunity to work under his supervision.

I would like to thank my family, to whom I have dedicated this thesis. Without their support, this work would have been impossible. I will always be in debt for their never ending love, support and encouragement. Finally, my thanks go to my wife for always being beside me and giving me motivation to move forward.

To Jiayue and Oliver

Table of Contents

List of Figures

List of tables

Nomenclature

BCF	Body and/or Caudal Fin
MPF	Medium and/or Paired Fin
AUV	Autonomous Underwater Vehicle
Y_{body}	transverse displacement of the tail unit
x	displacement along the tail axis
K	wave number
λ	wave length
C_1	linear wave amplitude envelop
C_2	quadratic wave amplitude envelop
f	frequency in Hz
ω	frequency in rad/s
AR	aspect ratio of fin
a	phase difference between the lead-lag motion and the feathering motion
b	fin chord length
s_c	fin area
β_i	phase angle

A_i	amplitude parameters of the *i-th* tail link
α	turning factor
k_l, k_r	control parameters for pectoral fin motion
A_ψ , A_φ	amplitude parameters for pectoral fin motion
F_u	thrust force generated by fish tail
F_r	moment generated by fish tail
x, y	coordinates of local frame of reference
X, Y	coordinates of inertial frame of reference
BL	body length
DOF	degree of freedom
U	swimming speed
R_t	length ratio
l_i	length of *i*-th link
θ_i	angle of the *i*-th link
φ_r	pitch angle of right pectoral fin
φ_l	pitch angle of left pectoral fin
ψ_r	yaw angle of right pectoral fin
ψ_l	yaw angle of left pectoral fin
$\boldsymbol{V}$	velocity vector of fish robot

u	forward velocity of fish robot
v	transverse velocity of fish robot
r	rotational velocity of fish robot
ψ	yaw angle of fish robot
x_c, y_c	fish robot center of mass position in global coordinates
a_i, b_i	curve fit parameters for normalized force and torque
P_i	parameters of robotic fish dynamic model
T_1, T_3	time constants for u and r velocities
τ_1, τ_3	normalized force and torque

1. Introduction

In recent years, there has been growing interest in robotic research where robots are either used to address specific biological questions or directly inspired by biological systems. A variety of biomimetic robots, ranging from flyers to swingers to swimmers, have been constructed. R. D. Beer and H. J. Cheil [1] give an overview of robotics research in their article on biorobotics. In the category of swimming robots, the development of biomimetic robotic fish is motivated by a desire to create Autonomous Underwater Vehicles (AUVs) with the virtues of being efficient, manoeuvrable and noise-free. Moreover, it provides essential insights into the mechanism and control of fish swimming [2].

1.1 Motivation

A fish in nature propels itself by the coordinated motion of its body, fins, and tail. This provides tremendous propulsive efficiency and excellent manoeuvrability compared to conventional marine vehicles powered by rotary propellers for the same level of power consumption. Swimming efficiency of an ordinary fish is over 80 percent, and fish in carangiform motion (see Fig. 2) can be up to 90 percent efficient [3]. However, the efficiency of a conventional screw propeller is only between 40 and 50 percent [53]. Dolphins are a good example of the speed and manoeuvrability that can be achieved using fish like propulsion. They can cruise at 20 knots and then can attack their prey with $20g$ acceleration when hunting for food. Furthermore, fish can turn rapidly with a radius of 10 to 30 percent of their Body Length (BL), while conventional ships turn

slowly with a radius of three times the BL [5]. From an engineering perspective, a fish is a distinguished AUV system that is well suited for mechanical reproduction.

1.2 Literature Review

Significant research work in robotic fish systems was initiated in the 1990s by Triantafyllou [5] and was further investigated by Hirata [6]. This was supported by rapid progress in robotics, hydrodynamics, materials, actuators, and control technologies. Current research has increasingly focused on the design and development of robotic fish. Apart from its significance as a research subject in robotics and its practical applications, robotic fish can be potentially be utilized in military systems, undersea operation, oceanic exploration, pollution detection, and many other applications.

The main fish swimming types are presented in Fig. 2. The following well established classification scheme and nomenclature was originally proposed by Breder [11]. Fish swim either by Body and/or Caudal Fin (BCF) movements or using Medium and/or Paired Fin (MPF) propulsion. The latter is generally employed at slow speeds, offering greater manoeuvrability and better propulsive efficiency, while BCF movements can achieve greater thrust and acceleration. For both BCF and MPF locomotion, specific swimming modes are identified based on the propulsion and the type of movements (oscillatory or undulatory) employed for thrust generation. In previous research, few robotic fish prototypes have been able to realize both BCF and MPF motion at the same time and there are few corresponding motion control methods.

There is an extensive body of literature on research related to robotic fish. The first robotic fish, RoboTuna, was developed at MIT in 1994 [42]. The main purpose of

this research was to study the hydrodynamics of fish swimming. The construction of RoboTuna was based on an eight-link aluminum skeleton covered by a smooth flexing Lycra hull. The tail was powered by six brushless motors. Several flow sensors installed on each side of the RoboTuna recorded flow pressure. After the RoboTuna was constructed, many other types of robotic fish were developed. At Northwestern University a robotic lamprey eel was developed using shape memory alloy actuators with the application aimed at mine countermeasures [12]. Nagoya University developed a micro robotic fish using ICPF actuators [13] and Tokai University constructed a robotic Blackbass for research on pectoral fin propulsion [14]. A robotic fish known as the Boxfish was developed at the University of California [15]. The particular focus of this work was a series of tests for comparing the effects of tail frequency when different materials were used for the tailfin. It was found that the fish speed increased not only with higher frequencies, but also with the increasing flexibility of the tailfin material. The results of these tests provide a valuable guide for understanding material properties and their influence on swimming performance.

From the existing research it is apparent that there are design and performance compromises when only one swimming motion is used to perform more than one task. For instance one mode might be better for low velocity motion [14], one mode better for high speed forward motion[11], and another mode might be better for high acceleration turning [4]. If only one mode is used for all these functions there will be significant performance trade-offs. However, fish that employ different propulsion modes for different tasks do not show significant performance compromises [16]. For example, fish that employ MPF motion in addition to BCF motion have a greater degree of control and

higher accuracy during low velocity manoeuvres than fish that just employ BCF propulsion [17]. Many underwater tasks such as inspection involve stationary positioning which is well suited to MPF propulsion. However, efficient high speed mobility is required to bring the fish robot into proximity to their work, which is better suited to BCF propulsion. Therefore, it is desirable to have both modes of propulsion for a robotic fish. This is one of the primary motivations for the novel robotic fish design proposed in this thesis that combines both BCF and MPF modes of operation. This concludes the overview in this chapter of research literature related to robotic fish design. A more detailed literature review of robotic fish propulsion and design approaches is presented in Chapter 2.

1.3 Thesis Objectives and Contributions

The main objective of this thesis is to develop a novel robotic fish that allows both BCF and MPF modes of operation to be investigated. This will provide a useful and interesting experimental framework for research related to dynamic modelling and control of robotic fish that employ both modes of operation. Very few robotic fish designs and prototypes have been developed to date with this capability, so it is expected that the novel design will allow new modelling and control techniques to be investigated in the future. The proposed design is based on a multi-link flexible tail structure for BCF motion with three degrees of freedom actuated by radio control servo motors. For the MPF motion, a pair of pectoral fins with yaw and pitch control is employed for each side of the fish. These two degrees of freedom are driven individually by radio controlled servo motors. It should also be noted that the robotic fish has a constant buoyancy, so it is restricted to two dimensional motion with no change in swimming

depth. A prototype of the new design is constructed and experimental tests are performed using an overhead vision system for position and orientation measurement. Based on the experimental data a low order dynamic model is developed. Finally, a next generation robotic fish design is developed based on the experience with the first prototype.

This thesis is organized as follows. In Chapter 2, the morphology of fish propulsion and a review of recent research on robotic fish designs is presented. The design of the proposed robotic fish and a description of the prototype is presented in Chapter 3. Experimental tests of the prototype are presented in Chapter 4 and a low order dynamic model is developed. A next generation fish design is proposed in Chapter 5. Conclusions and future work are discussed in Chapter 6.

2. Fish Morphology and Robotic Fish Design

This chapter provides an overview of fish morphology and research on previous robotic fish designs. This information forms a useful background in the design of the proposed fish robot in the following chapter.

2.1 Morphological Features of Fish Propulsion

The main properties of water as a locomotion medium, which have played an important role in the evolution of fish, are its incompressibility and its high density. The density of water (about 800 times that of air) is sufficiently close to that of the body of marine animals to nearly counterbalance the force of gravity. This allows the development of a wide variety of swimming propulsors, as weight support is not of primary importance [7].

The terminology to identify the fins and other features of fish that are most commonly found in the literature and used throughout this thesis are shown in Fig. 1. Median and paired fins can also be characterized by the length of the fin's base relative to the overall fish length. The fin dimensions in normal position and parallel to the water flow are called span and chord respectively [16].

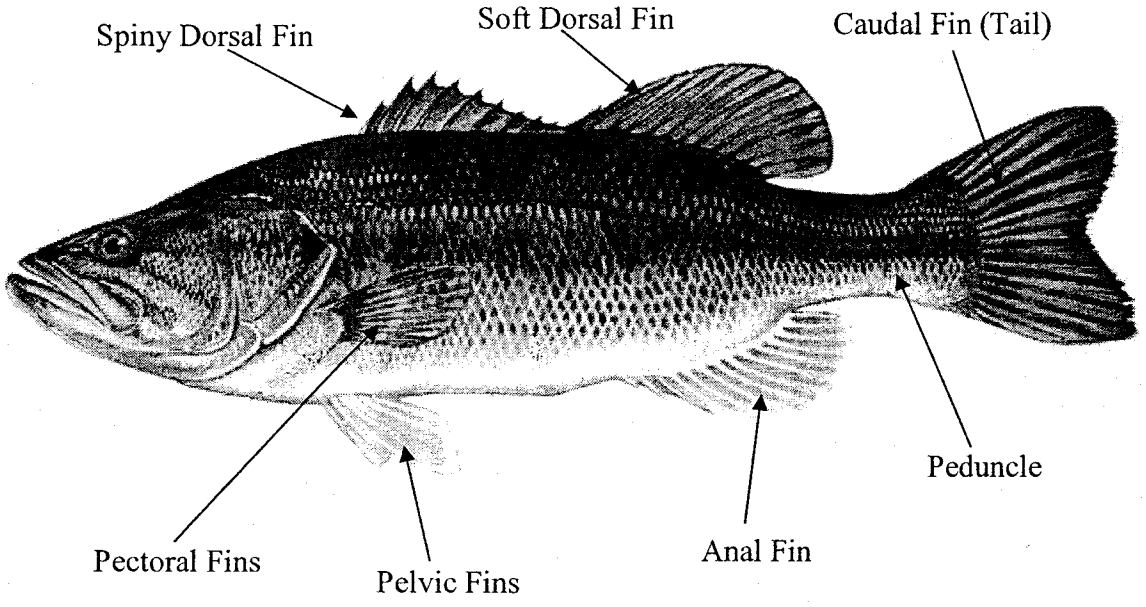

Fig. 1. Basic morphological features of a fish [2].

2.1.1 Forces and Motion

Swimming involves the transfer of momentum between the fish and the surrounding water. The main momentum transfer mechanisms are drag, lift and acceleration reaction forces. Swimming drag can happen in three ways:

- Skin friction between the fish and the boundary layer of water (viscous or friction drag). Friction drag depends on the wet area and swimming speed of the fish, as well as the nature of the boundary layer flow.
- Pressures formed in pushing water aside for the fish to pass (form drag). Form drag is caused by the distortion of flow around solid bodies and depends on their shape. Most of the fast-cruising fish have well streamlined bodies to significantly reduce form drag.

- Energy lost in the vortices formed by the caudal and pectoral fins as they generate lift or thrust (vortex or induced drag). Induced drag depends mostly on the shape of those fins.

The last two listed items are jointly described as pressure drag. Comprehensive overviews of swimming drag and the adaptations that fish develop can be found in [8] and [17].

Lift forces originate from water viscosity and are caused by asymmetries in the flow velocities. As fluid moves past an object, the pattern of flow can result in pressure on one lateral side that is greater than that on the opposite side. Lift is then exerted in a direction perpendicular to the flow direction.

Acceleration reaction is an inertial force generated by the resistance of the water surrounding a body or fin when the velocity relative to the water is changing. Different formulas can be used to estimate acceleration reaction depending on whether the water is accelerating and the object is stationary [17]. Acceleration reaction force is more sensitive to size than lift or drag, and it is especially important during periods of unsteady flow and fish movements [18], [25].

The main forces acting on a fish swimming are weight, buoyancy, and the forces due to the hydrodynamic momentum transfer mechanisms mentioned above. For negatively buoyant fish, hydrodynamic lift must be generated to supplement buoyancy and balance the vertical forces to prevent from sinking. Many species of fish achieve this by continually swimming with their pectoral fins extended. However, since induced drag is generated as a side effect of this technique, it disturbs the balance between horizontal forces, calling for further adjustments for the fish to maintain a steady swimming speed.

For a discussion on this coupling of the forces acting on a swimming fish see reference [16]. For a fish propelling itself at a constant speed, the momentum conservation principle requires that the forces and moments acting on it to be balanced. Therefore, the total thrust it exerts against the water has to be equal to the total resistance it encounters moving forward.

2.1.2 Classification of Swimming Movements

The classification of swimming movements presented here adopts the expanded nomenclature originated by Breder in [11]. Most fish generate thrust by bending their bodies into a backward motion propulsive wave that extends to its caudal fin, a type of swimming classified under Body and/or Caudal Fin locomotion (BCF). Other fish species have developed alternative swimming mechanisms that involve the use of their median and pectoral fins, termed Median and/or Paired Fin locomotion (MPF). Although the term "paired" refers to both the pectoral and the pelvic fins (Fig. 1), the pelvic fins (despite providing versatility for stabilization and steering purposes) rarely contribute to forward propulsion. Therefore, they are not associated with any particular locomotion mode in the classifications schemes found in research literature. An estimated 15% of the fish families use non-BCF modes as their routine means of propulsion, while a far greater number that rely on BCF modes for propulsion employ MPF modes for manoeuvring and stabilization [27].

There are also significant differences between fish species that relate to the specific mode of swimming movements used for different objectives. Webb [18] identified three basic optimum designs for fish morphology, derived from specializations

for accelerating, cruising, and manoeuvring operations. Since those specializations are largely mutually exclusive, no single fish exhibits an optimal performance in all three functions. However, fish species are not normally specialists in a single objective. They instead are propulsion generalists, combining design elements suitable for multiple objectives to varying degrees of optimality.

For the basic grouping into MPF and BCF propulsion, different modes of swimming can be identified for each group using Breder's [11] original classification and nomenclature scheme (Fig. 2). These modes can considered as specific motion patterns. However, it is possible to have motion that fall between these distinctive patterns. Fish can also exhibit more than one swimming mode, either at the same time or at different speeds. Median and paired fins are routinely used together to provide thrust with varying contributions from each, achieving very smooth trajectories. Further, many fish types typically utilize MPF modes for foraging, as it offers greater manoeuvrability, and switch to BCF modes at higher speeds and acceleration rates.

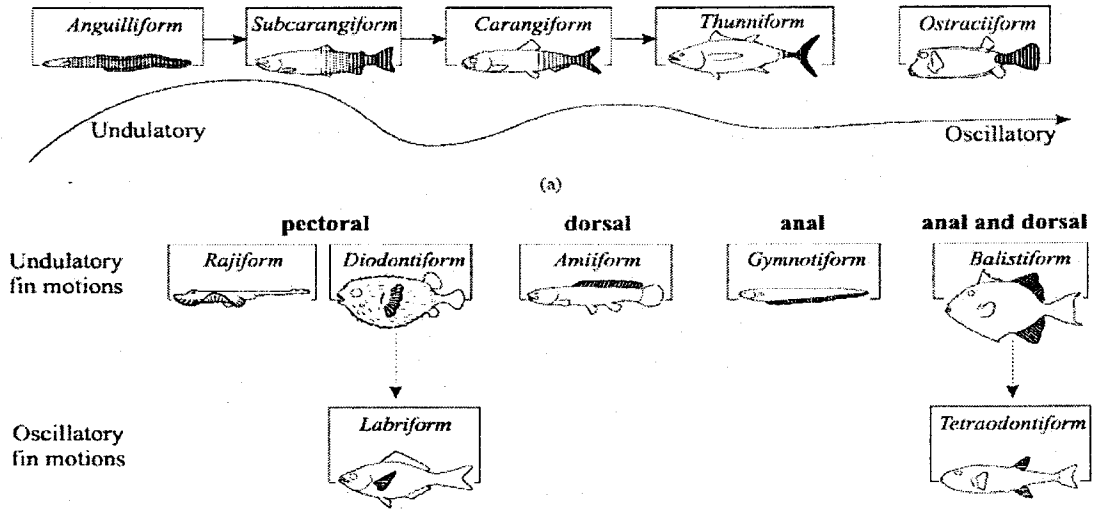

Fig. 2. Basic swimming models based on the studies of Breder [11].

2.1.3 Body / Caudal Fin Propulsion

In undulatory BCF modes, the propulsive wave moves through the fish body in a direction opposite to the overall movement at a speed greater than the overall swimming speed. The four undulatory BCF locomotion modes are identified in Fig. 3. They indicate changes mainly in the wavelength and the amplitude of the propulsive wave, and also the way thrust is generated. Two main physical mechanisms have been identified: an added-mass method and a lift-based (vorticity) method [11].

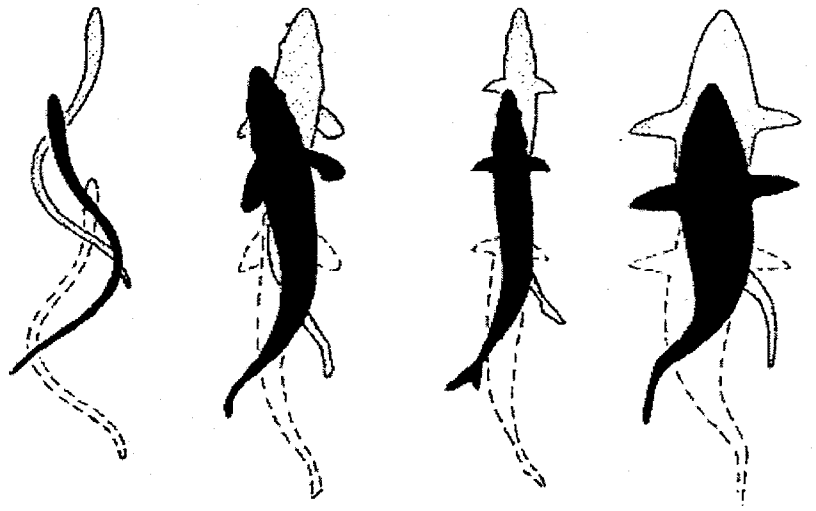

(a) (b) (c) (d)

Fig. 3. Gradation of BCF swimming movements: (a) anguilliform, (b) subcarangiform, (c) carangiform, and (d) thunniform mode [7].

2.1.4 Median / Paired Fin Propulsion

Fin oscillations usually involve median or paired fins. In labriform swimming, propulsion is achieved by oscillatory movements of the pectoral fins [11]. Swimming using the pectoral fins is widespread among teleost fish, and it has only recently received

more attention by the research community. This is due to the difficulty of observing and analyzing the fin kinematics as a result of the speed, variability, and complexity of the movements performed (flapping, rotating and undulating), as well as the transparent appearance of the fin membrane.

Blake [26],[34] identified two main oscillatory movement types for pectoral fins: (i) a rowing action (drag-based labriform mode) and (ii) a flapping action, similar to that of bird wings (lift-based labriform mode). According to Vogel [33], drag-based methods are more efficient at slow speeds, when the chord-wise flow over the fin is small, while lift-based methods are more efficient at higher speeds. Later research [34],[35],[36] emphasized the importance of acceleration reaction in thrust generation. It also indicated that pectoral fin movements are usually very complicated due to the highly flexible character of the membrane and the fin-rays. Complexities also include hydrodynamic interactions of the fins with the moving water and the fish body. Therefore, fish rarely exhibit a clear rowing or flapping movement. Instead, they use a combination of both that generally varies with speed.

Undulations are also often passed along the fins, and a large number of different types of movements can generate thrust in almost any direction allowing a high degree of manoeuvrability. The complexity of the pectoral fin motions is illustrated in the detailed 3-dimensional kinematic data made available recently in [30]. Reviews of pectoral fin swimming can be found in [29]. To understand the basics mechanisms of thrust generation in pectoral fin movements the studies of pure drag and lift based labriform locomotion can be used with the advantage of being more mathematically tractable. The fins normally have a short base that forms a large angle with the main axis. Their rowing

action consists of two phases: the power stroke, when the fins move posteriorly perpendicular to the body at a high angle of attack with a velocity v greater than the overall swimming speed U (see Fig. 4a), and a recovery stroke, when the fins are feathered to reduce resistance and brought forward (Fig. 4b). Thrust is generated through the drag produced as the fin is moved posteriorly and the acceleration reaction of the water being rapidly moved at the initial part of the power stroke. Since thrust is only produced during the power stroke, it is discontinuous and intermittent. This is different than the case for BCF propulsion, where thrust force is generated over most of the tail oscillation cycle.

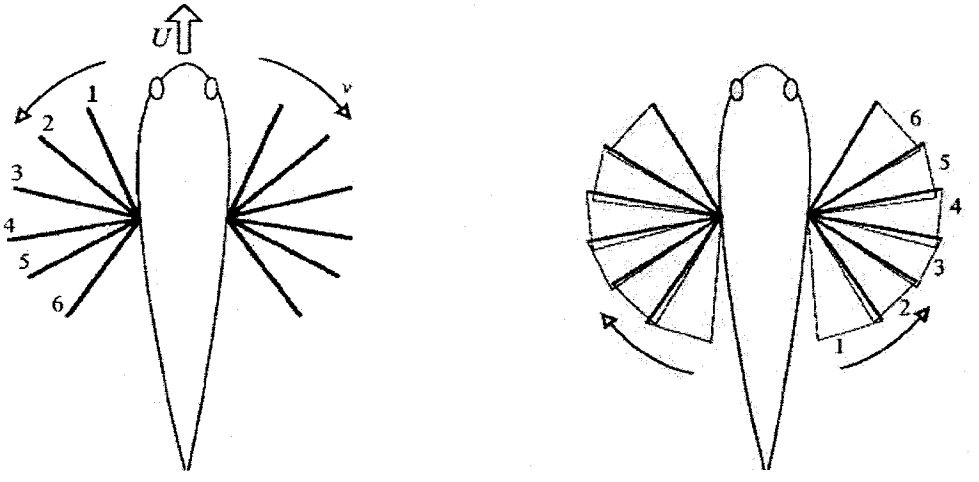

(a) Power stroke (b) Recovery stroke

Fig. 4. Diagram showing fin positions and angles of attack during (a) power stroke and (b) recovery stroke.

2.2 Review of Robotic Fish Designs

Most approaches to robotic fish design and construction originate from the engineering research community. Some researchers are searching for a new means of propulsion for ships and underwater vehicles. Others want to verify theoretical hydrodynamics models under realistic conditions in test tanks. The robotic designs in most recent research imitate real fish in their swimming modes, but there is still a large gap between the performance of these robots and a real fish. This section gives an overview of some of the most prominent robotic fish design projects over the last several years. A summary of this work is given in Table 1.

Project Name	Brief description	Mechanism	Year Initiated
RoboTuna I, II, MIT [45]	Thunniform fish designed to develop better propulsion systems for autonomous underwater vehicles. Design optimized for speed.	8 joints	1994
Robot Pike, MIT [4]	Design optimized for agility and high acceleration turning with the objective of a small low energy consumption autonomous underwater vehicle.	3 joints	1994
Robot B1, MIT [19]	Uses actual frog muscles for propulsion in a glucose solution (0.15 m length).	2 muscles	2001
PF600, NMRI [20]	Thunniform fish design for studying basic propulsion performance, operated by radio control (0.6 m length, 0.4 m/s speed).	3 joints	1998
PF700, NMRI [21]	Designed for high speed swimming, operated by radio control (0.7 m length, 0.7 m/s speed).	3 joints	2000

UPF2001, NMRI [22]	Designed for high performance and multiple objective use. (1 m length, 0.97 m/s speed).	1 joint with orientation control	2001
G1,G2,G3,G4, G5 and MT1, University of Essex (UK)	Fish robots that closely mimic fish propulsion and navigate autonomously.	2-5 joints	2003
BASS-II, N. Kato (Japan) [14]	Uses 2 pectoral fins to stabilize the fish robot.	2 pectoral fins	2000
Boxfish, University of California [15]	Micro vehicle controlled by piezoelectric bimorph actuators (12 mm length, 1 g mass).	2 joints for roll, 1 joint for yaw	2000
SPC-II, Beijing University of Aeronautics and Astronautics[24]	Semi-autonomous underwater vehicle (0.6 m length, 1.5 m/s speed)	2 joints for yaw direction	2004

Table 1. Brief overview of robotic fish designs.

The first RoboTuna was built in 1994 at MIT with the principal purpose of studying the hydrodynamics of fishlike swimming [45]. It consists of an eight-link aluminum skeleton covered by a smooth flexing Lycra hull and a tail powered by six brushless motors. One single strut encloses all of the cables for power and data. Depending on the research topic, several pressure sensors were placed at different points along the body. The fish was put into a tow tank for testing and studying various hydrodynamics propulsion principles. This lead to a new free swimming propulsion model. One of the other research topics investigated is flow control. Several flow sensors installed on each side of the RoboTuna recorded flow pressure. The fine-scale pressure

variations that occur between two vortices was measured and used to directly influence the control of the motors and tail movement in response to vortex formation [43].

A difficult problem in fish robotics research is the development of mechanical devices that emulate the complex attributes of muscle motion. Mechanical power sources (motors, pneumatics, etc.) need to be appropriately transformed by complex mechanisms to achieve good approximations of continuous swimming motion. However, this often leads to additional energy loss in the mechanism. In [44], different mechanisms were calculated and proposed that should mimic as closely as possible a predefined path for the trailing edge of the tail fin. One particularly noteworthy aspect of this work is the test series on materials used for the tailfin, which demonstrated that speed increased not only with higher frequencies, but also with the increasing flexibility of the material. The study in [51] compares a tuna type tailfin to a pike type tailfin. It shows that the tuna type tailfin is more suitable for high-speed swimming in a high frequency range. This case illustrates the problem of parameter optimization, despite using only two degrees of freedom.

The SPC-II robotic fish design can be placed between the RoboTuna and the Boxfish [49]. While the construction is not as complicated as RoboTuna (which has 8 joints), it is not a drastic simplification of swimming motion which is employed in the Boxfish design. The SPC-II employs two degrees of freedom (three joints and two servomotors), which allows a wide range of behavioural diversity, yet it is simple enough to provide reliable test performances [24]. In [50], three different turning modes are investigated. In the first mode, the head part of the fish robot is used as a rudder while the tail oscillates with an offset to its initial position. This mode is the primary swimming motion, because it is fast and it can be adjusted to work with various turning radii by

changing the offset. The smallest turning radius can be achieved by setting the offset to its maximum. In another turning mode, the fish robot starts from a stationary state. It then rapidly swings its tail to one side so that the body yaws until it comes to a stop or starts swimming forward. The advantage of this mode is that it achieves the smallest possible turning radius, approaching a turn in place motion. The disadvantage is the lack of direct control on the turning speed and angle.

While the RoboTuna emulates swimming motion using a complex eight joint mechanism, other researchers have developed designs that only use 3 or 4 joints [23]. This results in less morphological similarity to a real fish than a more complicated design, but it still provided fish-like swimming motions useful for control research objectives. Skin design and waterproofing is another significant challenge for robotic fish researchers. Some designs use flexible material with a solid frame. For example, Lycra fibre is used on Robot Tuna and Latex rubber is used on SPC-II. Other designs use a rigid hull, a sectioned rigid peduncle, and caudal fin like PF500/600/700 [14]. From this research it is evident that material properties and morphology have a strong influence on the kinematics and dynamics of fish motion and the interaction with the surrounding fluid. Therefore, these factors deserve careful consideration in the design process.

3. Design and Implementation of the Robotic Fish

The main objectives for the design was to develop a small low cost radio controlled robotic fish with both BCF and MPF propulsion that is capable of forward and turning motions in a small swimming pool environment. To address these objectives, a new robotic fish design is proposed in this chapter. The implementation of the swimming modes is discussed and the prototype of the new design is presented.

3.1 Swimming Methods of the Robotic Fish

3.1.1 Body / Caudal Fin Propulsion

The movement of a robotic fish mainly depends on how the tail joints rotate. The kinematics for the robotic fish tail joints determines if the robotic fish swims realistically and if the swimming motion is highly efficient. It also determines how much propulsion force is generated and what speed can be achieved. An idealized motion of a fish tail can be described using a traveling wave Equation (1), as originally suggested by Lighthill [2]. The origin point is at the junction between the fish head and tail. This swimming motion can be viewed as the generation of a traveling wave. The parameters of (1) are the key elements in determining the ideal kinematics of the fish tail.

$$y_{body}(x,t) = (C_1 + C_2 x^2)\sin(Kx + \omega t) \qquad (1)$$

where $y_{body}(x,t)$ is the transverse displacement of the tail, x is displacement along the main axis, $K = 2\pi/\lambda$ is the number of waves, and λ is the wave length. The parameter C_1

is the linear wave amplitude envelope, C_2 is the quadratic wave amplitude envelope, and ω is the wave frequency of the tail.

In a real fish, which has many vertebrae, each vertebra can be viewed as a small joint in order to approximate an ideal continuous wave. This leads to a very smooth approximation. However, a robotic fish only has a limited number of joints, making it impossible to generate a fully continuous and smooth fish-like wave. Determining how to use limited joints to approximate the traveling wave of a real fish is a major challenge for robot researchers. Considering the fact that the oscillatory part of a fish consists of many rotating hinge joints, it can be modeled as a planar serial chain of links along the body axis. The optimal position of each link in the moving chain can then be determined by numerical fitting to the idealized wave. Based on this information the shape of the fish tail can be changed geometrically by commanding different deflections $\Delta\theta_i$ of the joints. When this data is used to command the servo motors of the fish tail, the robotic fish will swim in a similar manner to a real fish. The more joints that are used the more realistic the approximation will be. It should be noted that the dynamics of the tail linkage will also be affected by the interaction with the water, a complex hydrodynamics interaction known as the added mass effect. In this thesis, it is assumed that the servo motors used (which employ closed loop position feedback) can compensate for this effect so that it may be neglected.

3.1.2 Median / Paired Fin Propulsion

In a similar manner to the beating motion of a bird's wings, the motion of pectoral fins on fish generally consists of four basic motions [27],[29]:

- flapping motion in the vertical plane
- lead-lag motion in the horizontal plane
- feathering motion, which involves a twisting motion of the pitch angle
- spanning motion, which involves alternatively extending and contracting motion of the fin span

Only the lead-lag motion in the *x-y* plane and the feathering motion in the *x-z* plane were employed in this thesis, since they are effective when combined and they can be implemented without too much mechanical complexity. The flapping motion that produces the vertical and spanning motions of the fish was also neglected because the robotic fish motion in thesis is restricted to the horizontal plane. The pectoral fins were also made sufficiently stiff so they can be treated as rigid plates.

The pectoral fin plate is made of plastic with a thickness of 1.2×10^{-3} m and a maximum chord length of 0.055 m. The lead-lag motion and the feathering motions are defined in Fig. 5. Fig. 6 defines the lead-lag angle ψ (yaw) and the feathering angle φ (pitch) for the right-hand side of the robot. Based on the intuitive understanding of MPF motion described in this section and in [27],[29] the following sinusoidal equations are proposed for the lead-lag and feathering angles

$$\psi = A_{\psi}\cos(2\pi ft) \tag{2}$$

$$\varphi = A_{\varphi}\cos(2\pi ft + a) \tag{3}$$

where A_ψ and A_φ are amplitude parameters for yaw and pitch, respectively. The angle a represents the phase difference between the lead-lag motion and the feathering motion and f is the frequency in Hz.

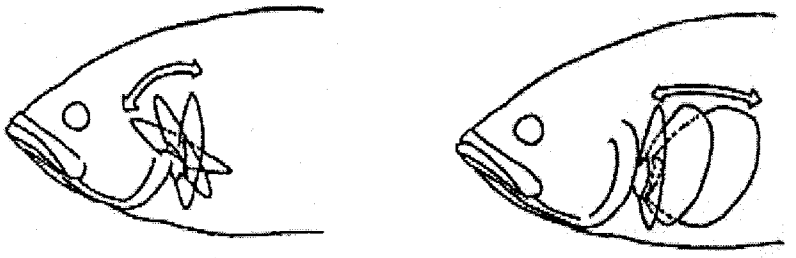

(a) Feathering motion (b) Lead-lag motion

Fig. 5. Definition of feathering motion and lead-lag motion.

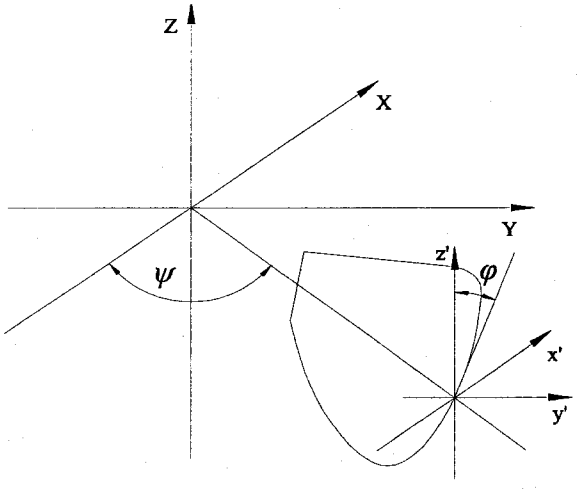

Fig. 6. Definition of lead-lag angle and feathering angle.

3.2 Mechanism Design

3.2.1 Body / Caudal Fin Mechanism

For BCF motion, a closed multi-link mechanism with two servo motors located at the base was employed (see Fig. 7). For achieving smooth fish-like motion, it is better to have as many joints as possible. However, in order to obtain a relatively simple structure, the robotic fish design has only three joints. The lunate foil is driven by three servomotors, with two of them attached to the fore-body and one of them attached to the last link (see Fig. 8). The installation position of the joint and the size of the tail are designed with consideration of the shape of a biological labriform fish model. This design has the advantage that it is relatively simple to construct, but also has low tail inertia and high stiffness since two of the motors are at the base and not on the moving tail linkage.

Aluminum fish ribs are used to support the latex skin of the fish tail and reinforce the structure of the tail. The schematic of the robotic fish ribs are shown in Fig. 7. All the ribs are attached to the tail linkage and will turn freely with the tail. The structure of the fish fore-body consists of a rigid aluminum and plastic frame that is covered by rubber. A flexible lunate caudal fin is attached to the last link and used as the tail fin. The installation position of the joint and the size of the tail are also designed with consideration of biological fish dimensions. A 30 inch latex balloon is used as skin to cover the fish tail, providing a lightweight and very flexible tail surface. Rubber and latex are used as skin to cover the body and make the tail flexible.

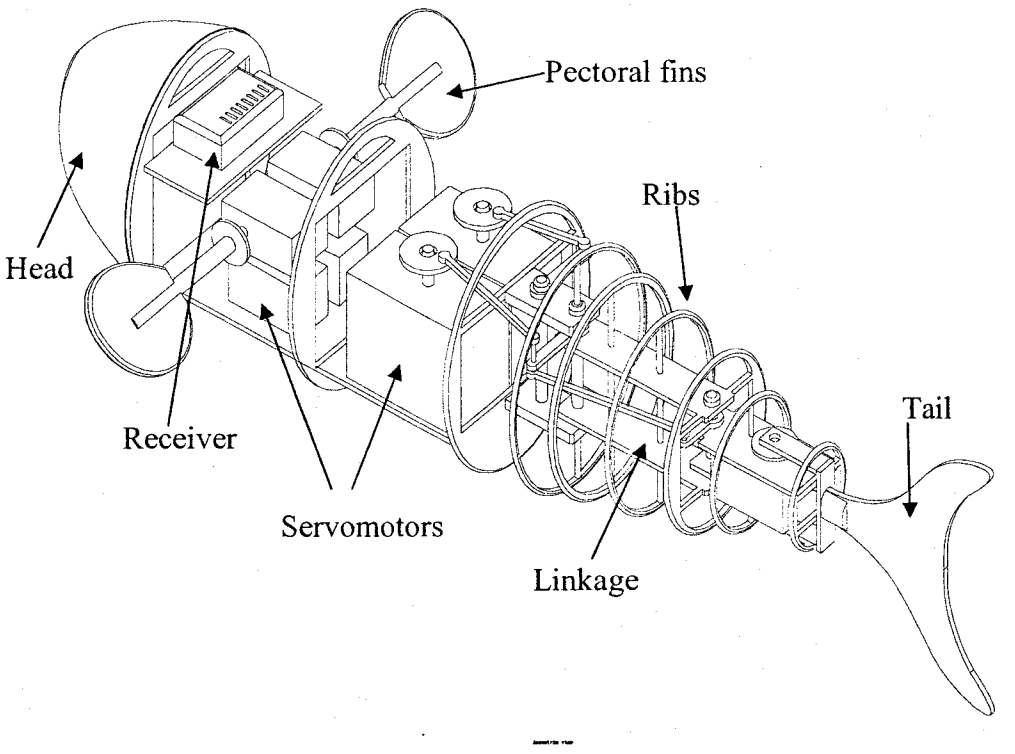

Fig. 7. Mechanical configuration of the robotic fish.

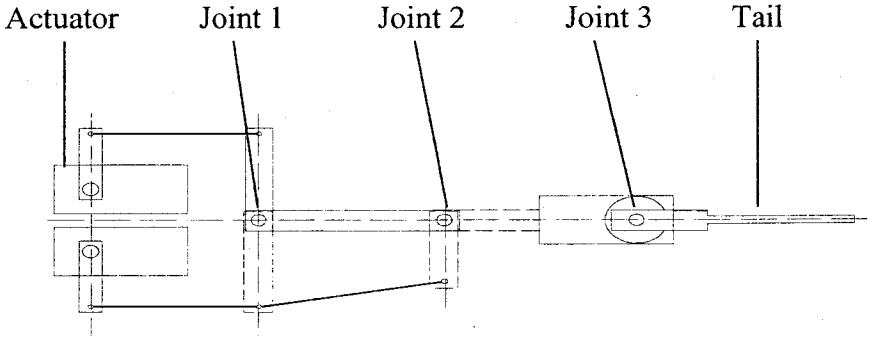

(a)

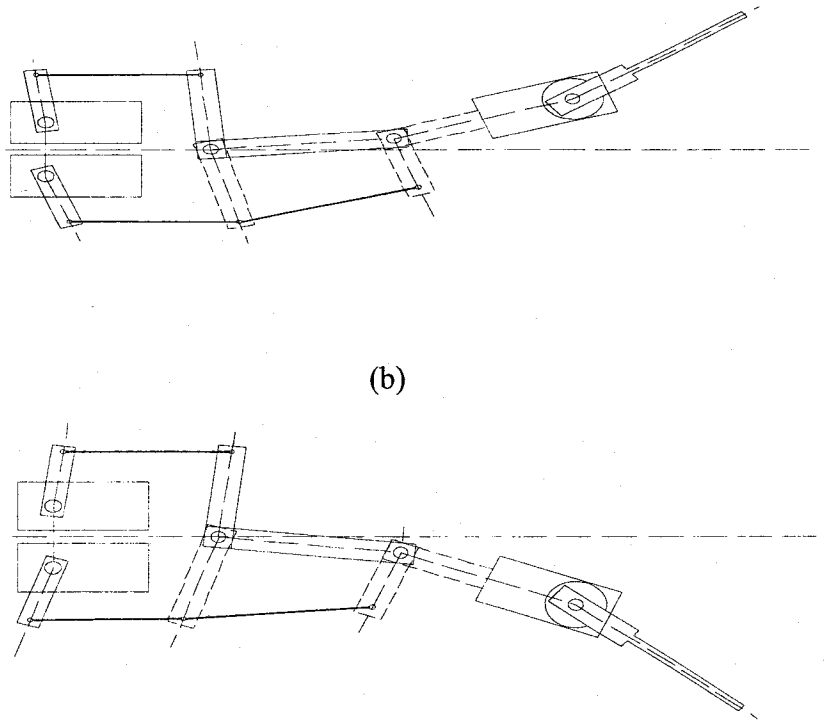

(b)

(c)

Fig. 8. Illustration of the linkage kinematics of the robotic fish: (a) neutral position of tail, (b) right position of tail, and (c) left position of the tail.

3.2.2 Median / Paired Fin Mechanism

The robotic fish design is equipped with a pair of pectoral fins driven by two servomotors each that are fixed inside the fore-body (see Fig. 7). The two servomotors generate the lead-lag motion (yaw) and the feathering motion (pitch) of a pectoral fin (Fig. 9). This design has the advantage that it is simple and compact since there is no linkage employed. The sinusoidal inputs proposed in (2-3) can be readily achieved using the proposed design.

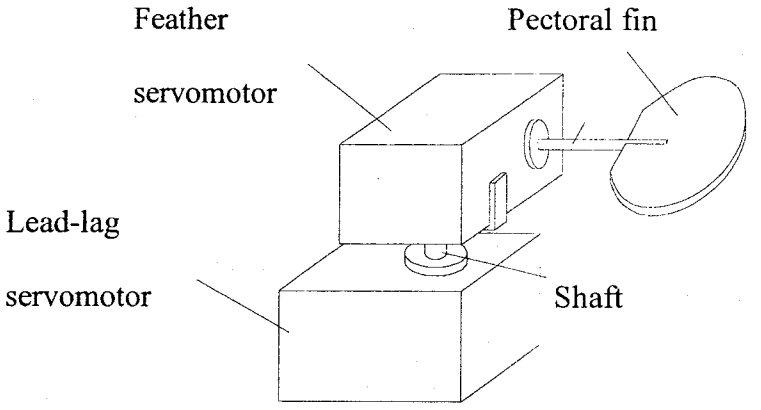

Fig. 9. Schematic view of robotic fish pectoral fins.

3.2.3 Length Ratio Specification

The length ratio R_l is defined as the length of the oscillatory part of the tail over the length of the fish body. Depending on the different values of R_l, fish swimming can be classified as carangiform, anguilliform, and thunniform. With a decrease in R_l, the efficiency and velocity of fish swimming increases, but manoeuvrability is reduced. In the proposed robotic fish design, the body length is 0.550m and the oscillatory part is 0.250m, so the ratio R_l is 0.454. This is considered to be a suitable ratio to balance manoeuvrability and cruising ability. In the parts of the robotic fish where the linkage lengths are relatively short, the density of the joints is high and the flexibility of produced motion is large, so that large-amplitude oscillation can be produced. As a general rule, the length ratio of each link moving from the nose to the tail of the fish should get smaller and smaller. The oscillatory amplitude increases gradually and reaches its maximum at the end of the tail.

3.2.4 Caudal and Pectoral Fin Characteristics

The aspect ratio (AR) of the caudal fin plays an important role in propulsive efficiency. It is defined as the fin chord length b squared, divided by the projected fin area s_c:

$$AR = b^2 / s_c \tag{4}$$

A high AR value for the caudal fin results in improved efficiency, since it induces less drag per unit of lift or produced thrust. Further, the shape of the caudal fin makes a large difference in fish propulsion. A crescent or forked caudal fin will normally be well suited for high-speed swimming. In the robotic fish design, a lunate caudal fin is used in which the fin span b is 0.1 m and the projected fin area s_c is 0.0066 m^2. The aspect ratio for this case is 1.515. The dimensions of the caudal fin are shown in Fig. 10(a). The pectoral fin design is a rigid flat plate made of plastic. The dimensions of the pectoral fin are shown in Fig. 10(b). The pectoral fin span is 0.051 m and the chord length is 0.05 m, making the projected fin area s_c=0.002065 m^2. The aspect ratio of the pectoral fin is therefore 1.259. For both the caudal and pectoral fins, the aspect ratios are relatively large which helps improve the efficiency of the swimming motion.

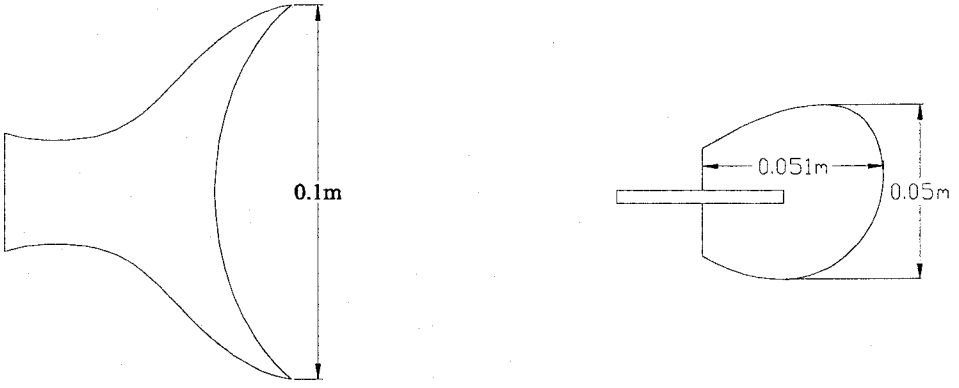

(a) (b)

Fig. 10. Dimensions of mechanical fin: (a) tail fin and (b) pectoral fin.

3.2.5 Body Structure and Fish Skin

Based on hydrodynamics principles, a hollow streamlined rigid head and fore-body were selected for the fish design (see Fig. 7) which in turn were covered with rubber. This shape while being relatively efficient allows for more space to house the electrical motors, battery, and communication components. Steel balance weights are located in the fore-body and the lower side of the tail to balance the gravitational force with the buoyant force, thus allowing two dimensional fish motion close to the water surface. In order to be able to swim in a small experimental swimming pool, the robotic fish must be as compact as possible. The head of the robotic fish is made from moulded hot-melt glue and reinforced by a plastic plate. The fore-body is divided by three plastic bulkheads that both create watertight compartments for containing water in the case of a hull breach/leak and increase the structural rigidity of the robotic fish. Bracing rods were added to join the bulkhead together and support the rubber skin of the hull.

Choosing the material of the fish skin is a major problem of robotic fish design, because the skin must be very flexible and have high expandability to help the fish tail move freely. Many materials were tested (rubber, leather, textile, etc) and finally a large 48 inch latex balloon was chosen as the skin to cover the tail. Since the latex balloon is very soft, some metal reinforcing ribs are attached to the tail vertebra in order to preserve the shape of the fish tail and protect the actuators inside.

3.3 Prototype Construction

Based on the proposed design a prototype robotic fish was constructed (see Fig. 11). The unwrapped robotic fish prototype is shown in Fig. 12 and the design schematic is shown in Fig. 7. The prototype uses radio controlled servos that can be controlled from a personal computer. The wireless receiver, battery, and seven servomotors were placed in the cell of the fish fore-body and sealed by silicone to prevent water leakage. The robotic fish primarily consists of:

- Communication unit (radio transmitter and receiver)
- Mechanical structure (aluminum frame/ribs, head, and fore-body)
- Actuator unit (seven DC servo motors and a rechargeable battery)
- Tail fin and pectoral fins
- Waterproof skin

In addition to the robotic fish, the experimental system also includes a personal computer, overhead web camera, data acquisition card (Quanser MultiQ), and radio transmitter (Hi-tech Laser 6). A control program on the personal computer realizes various motion

patterns for the robotic fish. The primary technical specifications of the robotic fish prototype are described in Table 2.

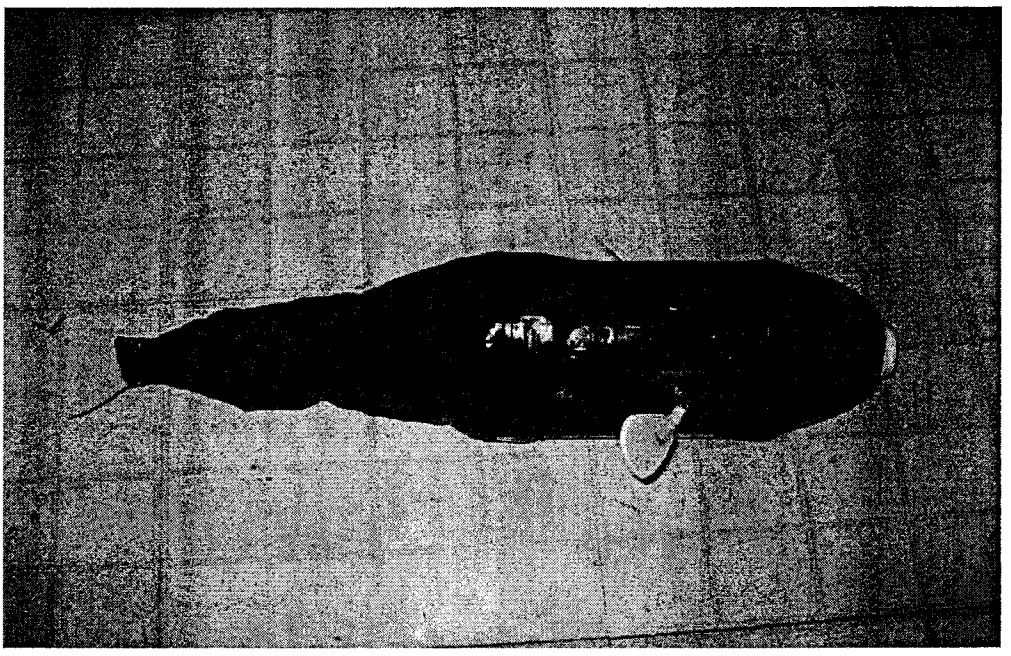

Fig. 11. Photograph of the prototype robotic fish.

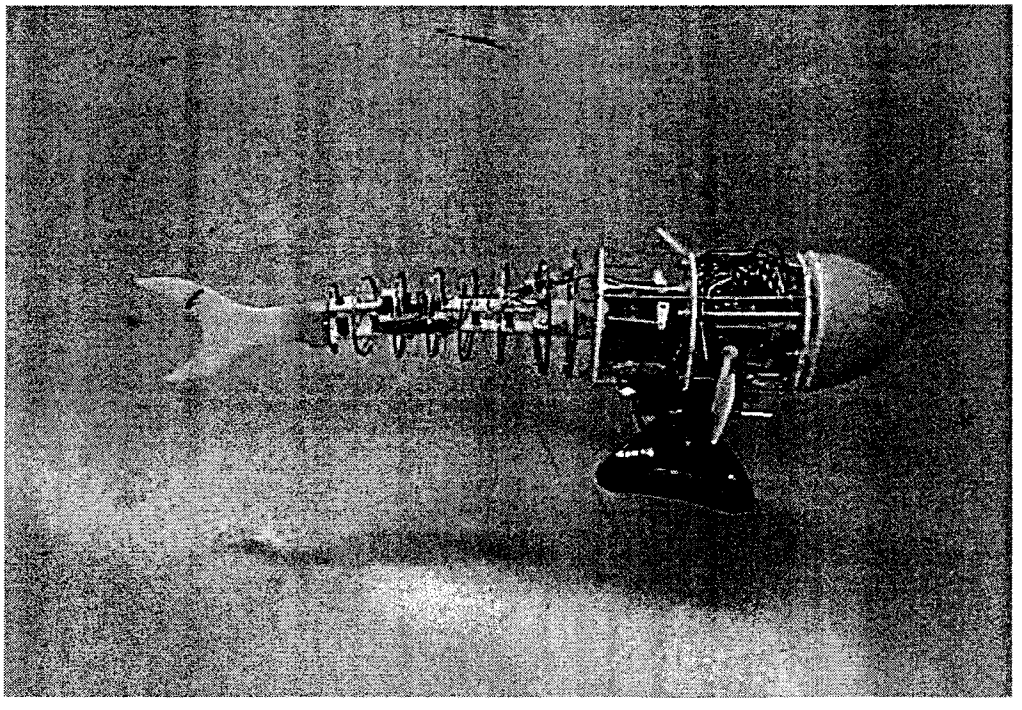

Fig. 12. Photograph of the unwrapped prototype robotic fish.

Body length	0.550 m
Mass	3.8 kg
Number of tail joints	3
Servomotors (2 tail joints):	Hitec HS-75BB
Number	2
Maximum torque	6.6×10^{3} kg/m
Servomotors (1 tail joint, 4 pectoral fins):	Hitec HS-422
Number	5
Maximum torque	3.3×10^{2} kg/m
Length of oscillatory part	0.260 m
Maximum speed (BCF)	0.151 m/s
Battery	4.6V NiMH rechargeable battery
Radio transmitter	Hitech Laser 6 FM radio with 6 channels

Table 2. Primary technical specifications of the robotic fish prototype.

3.4 Experimental Setup

The experimental setup is composed of a robotic fish, overhead camera, radio transmitter, swimming pool, and a personal computer (PC) with a data acquisition card. The PC sends voltage outputs from the D/A channels of the data acquisition card into the radio transmitter. These voltages are interpreted by the transmitter as desired position commands which it forwards to the receiver located on the fish robot. The receiver then sends the desired position commands to the servo motors. The servo motors use local position feedback controllers with potentiometer sensors to achieve the desired command positions. Therefore, the seven servo motors in the robotic fish can be controlled independently using a Visual C++ computer program. This allows the actuators to be given different position trajectories to achieve fish swimming motions.

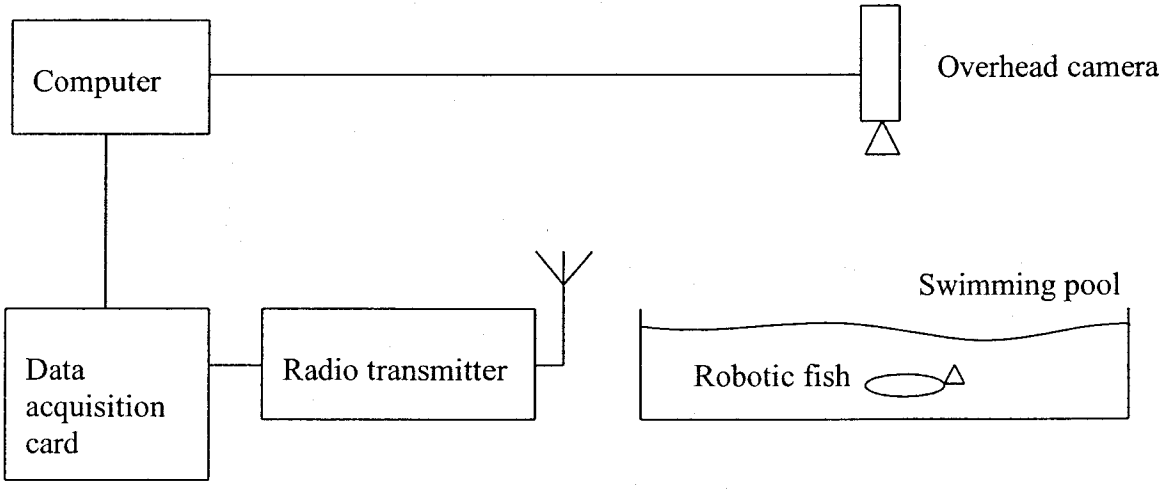

Fig. 13. Robotic fish experimental setup.

The fish robot does not have any local sensors. However, the overhead camera provides the capability for position and direction measurement of the fish robot. This

capability can be used either on-line (real-time machine vision) or off-line by recording video for later processing. For this thesis work, the experimental results are recorded as video and processed later to determine the position and orientation of the fish at different times. To implement a feedback controller, however, real-time machine vision would have to be used. The video was recorded using a resolution of 640×480 pixels with 24-bit colour at a frequency of 15 Hz. Colour information was used (via a simple image segmentation algorithm) to locate the centroids of a green target located on the fish head and a red target located on the fish body (see Fig. 11). This allows the position and orientation of the robot to be calculated for each frame of the video. Thus, the position and orientation of the fish could be determined at a frequency of 15 Hz. Together, the experimental apparatus allows the position of the servo motors on the robotic fish to be independently controlled and the position/orientation of the fish to be measured. Experiments using this setup are performed in the following chapter and a dynamic model of the robotic fish is developed.

4. Robotic Fish Modeling

In this chapter, a low order dynamic model of the robotic fish will be developed for the BCF fish motion in both the forward and turning modes of operation. The parameters of the model are also identified and the results are compared to experimental data. A brief study of the MPF fish motion is also presented.

4.1 Testing Environment

The experiments were performed in a swimming pool environment (see Fig. 14) with dimensions of 10 m x 5 m x 1.8 m. The walls and bottom of the pool were covered by blue ceramic tiles. The pool water had a small current due to circulation of the water through the cleaning filters. Light sources were placed on the ceiling to help improve the camera picture quality. During the experiments, video sequences were taken with a Logitech Quick-cam web camera mounted on the ceiling that was connected by a USB 2.0 interface to a computer. From the video sequences, the position and orientation of the fish robot was obtained at a sampling rate of 15 Hz by calculating the centroids of the red and green coloured targets on the robot (see Fig. 14).

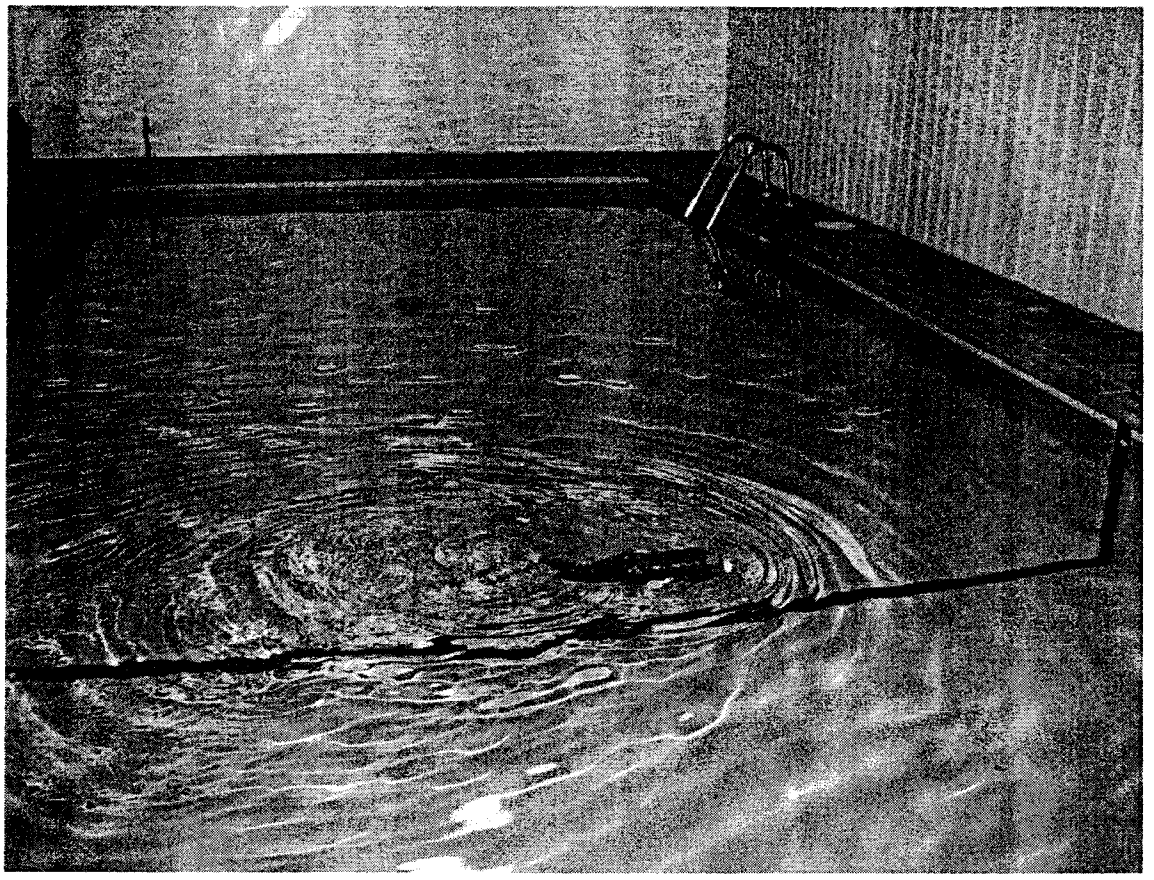

Fig. 14. Swimming pool used for robotic fish testing.

4.2 Actuation Process

The ideal kinematics of carangiform swimming motion in fish can be described by the following equation [2]

$$y_{body}(t) = (C_1 x + C_2 x^2)\sin(Kx + \omega t) \tag{5}$$

where y_{body}(t) is the transverse displacement of the tail, x is the position along the body axis, K is the body wave number, ω is the body wave frequency, C_1 is the linear wave amplitude envelope, and C_2 is the quadratic wave amplitude envelope.

In order to produce similar patterns of oscillation to carangiform swimming motion, the servo motors were given angle position commands for the i^{th} tail links (see Fig. 15) using the following proposed empirical equations.

$$\theta_i(t) = A_i(1 - \frac{|\alpha_i|}{2})\sin(2\pi ft + \beta_i) + A_i\frac{\alpha_i}{2} \quad , \quad i = 1,2,3 \tag{6}$$

where θ_i(t) is the oscillating set point (radians) for the i-th link, f is the tail frequency (Hz), and β_i is the phase angle (radians). The parameters A_i and turning factors α_i control the amplitude and offset of the oscillation, respectively. The turning factors α_i vary from -1 to 1. In this thesis, it is assumed that all the turning factors are equal so that $\alpha_i = \alpha$. When α equals 0 the robotic fish will swim forward without turning. It will turn right when α is negative and left when α is positive. Based on preliminary experimental optimization results, the phase angle β_i was selected as [0,π/4,π/2]. Due to mechanical constraints A_i was selected as [1.9π/10, 2.1π/10 , 2.5π/ 10].

Given the equation for θ_i(t) and the related parameters, different frequencies f and turning factors α will result in different trajectories for the link angles along with different forward speeds and turning rates for the fish. An illustration of the link angle trajectories for different values of f and α are shown in Fig. 16 and Fig. 17. For the model developed in this chapter two modes of operation were defined. Forward operation with $\alpha = 0$ and turning operation for $\alpha = 1$ and $\alpha = -1$. For each mode of operation the control input for the system is considered to be f. As this input is increased it normally results in higher forward velocity for the forward operation mode and faster turning rates for the turning operation mode.

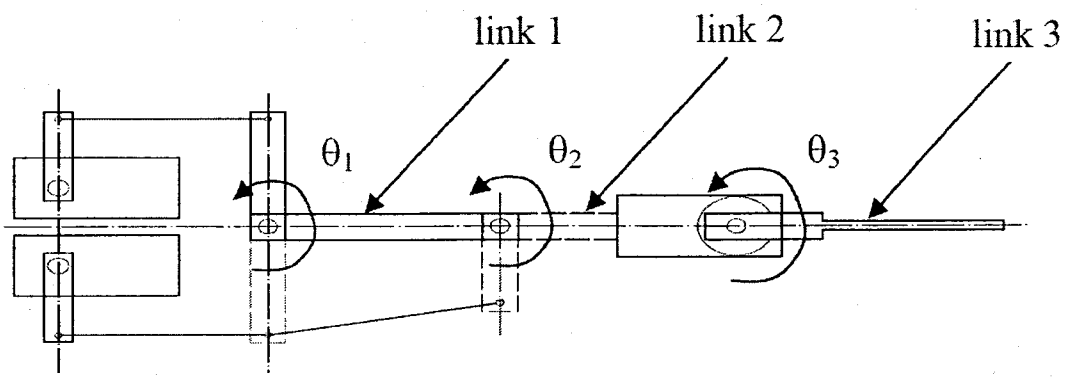

Fig. 15. The *i*-th tail links.

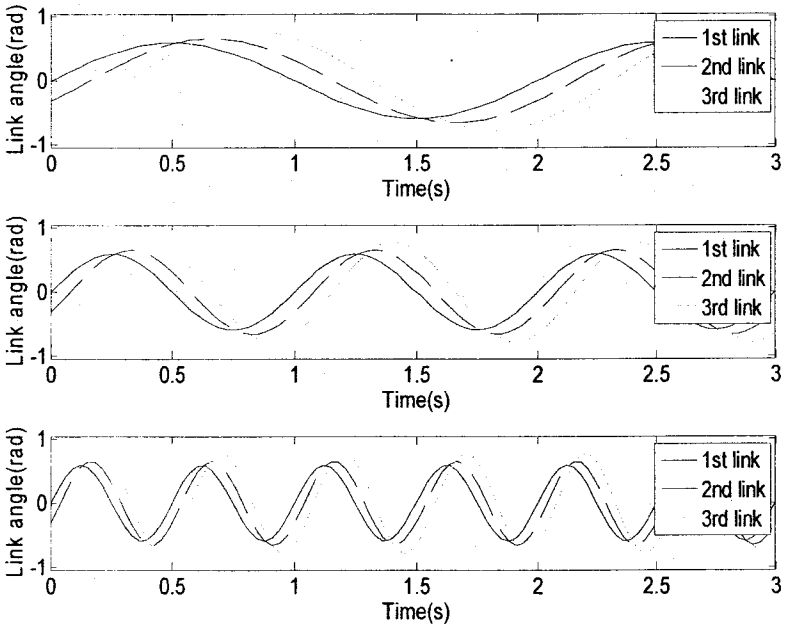

Fig. 16. Angle of *i-th* link for turning factor $\alpha = 0$ and frequencies (a) $f = 0.5$ Hz, (b) $f =$ 1 Hz, and (c) $f = 2$ Hz.

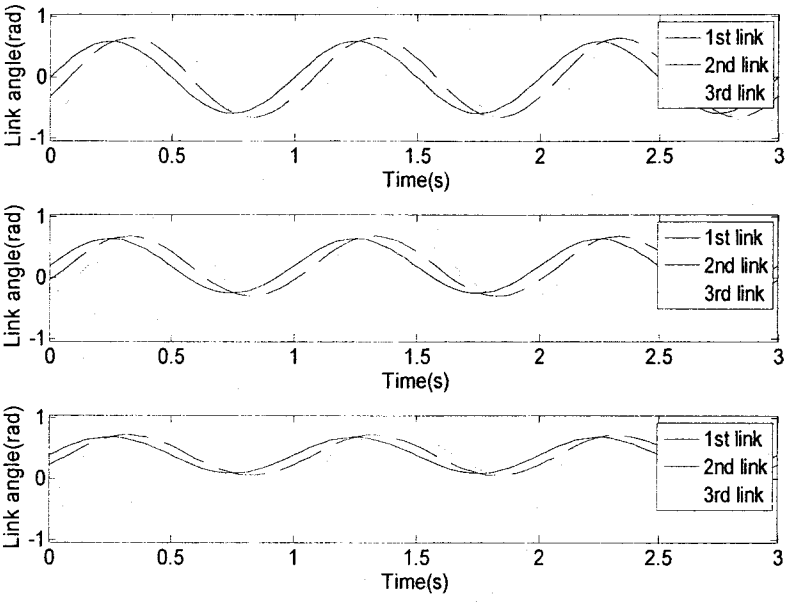

Fig. 17. Angle of *i-th* link for frequency f = 1 Hz and turning factors (a) $\alpha = 0$, (b) $\alpha = 0.5$, and (c) $\alpha = 1$.

4.3 Dynamic Model

In this section, a dynamic model of the robotic fish BCF swimming motion is developed for both the forward and turning modes of operation. In general, the dynamics of fish locomotion is very complicated due to the complex interactions between the robotic assembly in the fish tail and the fluid mechanics of the water. This results in unsteady water motion, vortices, and flow structure interactions. To fully model this behaviour would require a detailed computational fluid dynamics model which is not well suited for control applications. The complicated fine scale oscillations observed in the experimental data confirmed these notions. However, there did appear to be a bulk average motion of the fish similar to the motion of a marine vessel. To capture this behaviour a low order model was developed for the large scale bulk motions of the fish

robot. This type of model would not be useful for optimization of the fish motion. However, it would be potentially useful for analysis and design of trajectory controllers. The key assumptions for the proposed low order dynamic model are as follows:

1) The fish motion is restricted to two dimensional planar motion. The fish was designed with constant buoyancy and two dimensional control surfaces so that the depth of the fish would not change in the water. For the experimental tests the buoyancy was adjusted so that the fish just stayed beneath the surface of the water.

2) The rotational oscillations of the fish due to the body reactions from the tail oscillations are neglected. The direction of the fish is considered to be the average direction over one cycle of the tail oscillations. From the experimental data this was found to be a fair assumption even though the amplitude of the oscillations could be as large as 20 degrees or more. Improved robotic fish designs will be developed in the future to reduce this phenomena.

3) The actuation process is considered steady with respect to the oscillation cycle of the tail. The force and torque on the fish body are considered to be averaged over one cycle of the tail. In practice, this approximation was found to be good since the period of the tail oscillation is significantly smaller than the time constants of the forward speed and rotation rate. Therefore, the tail behaves roughly on average like a propeller that can change directions, while the body of the fish is like a marine vessel. This assumption is consistent with the previous assumption neglecting the fast rotational oscillations.

4) The bulk motion (the current) of the water is neglected. This was found to be a reasonable assumption in the experiments since the pool had only small currents associated with the water filtering. However, the effect was noticeable and for any significant water current this effect would have to be modelled.

5) Two modes of operation are modelled. This includes forward and turning modes, each with its own set of model parameters. Furthermore, the control input is considered to be only the oscillation frequency of the tail. This assumption was made to reduce the amount of experimental data needed to identify the model. If a significantly larger set of data was available the coefficients of the model could be identified for different turning factors α. A lookup table could then be determined and α could also be considered a control input.

Together, these assumptions lead to an idealized behaviour similar to the dynamics of a marine vessel. The dynamic model developed in this thesis is based on the low order control oriented model presented in [61]. This model was found to be effective for dynamic modelling and control of marine vessels undergoing mainly 2D motion on the surface of the water. A local body coordinate frame of reference is used to describe the motion of the system (see Fig. 18). The kinematic relation between the velocities in the local frame of reference and the position in the global frame of reference is given by

$$\begin{aligned} \dot{x}_c &= \cos(\psi)u - \sin(\psi)v \\ \dot{y}_c &= \sin(\psi)u + \cos(\psi)v \\ \dot{\psi} &= r \end{aligned} \tag{7}$$

where x_c and y_c represent the global coordinates for the center of mass, ψ represents the yaw angle, and r represents the yaw rate. The variables u and v represent the components of the inertial velocity V in the local x and y directions, respectively. The equations of motion in the body frame coordinates are given by

$$\dot{u} = \frac{m_{22}}{m_{11}} vr - \frac{d_{11}}{m_{11}} u + \frac{1}{m_{11}} F_u \tag{8}$$

$$\dot{v} = -\frac{m_{11}}{m_{22}} ur - \frac{d_{22}}{m_{22}} v \tag{9}$$

$$\dot{r} = \frac{(m_{11} - m_{22})}{m_{33}} uv - \frac{d_{33}}{m_{33}} r + \frac{1}{m_{33}} F_r \tag{10}$$

where m_{11}, m_{22}, and m_{33} are inertia matrix parameters. The damping matrix parameters are given by d_{11}, d_{22}, and d_{33}, respectively. The force in the forward direction is given by F_u and the torque in the yaw direction is given by F_r. This model neglects disturbance forces/torques and it also assumes a simple viscous friction model for interaction of the vessel with the water. However, it was found to be sufficient for design of tracking controllers for marine vessels. Equations (7-10) together form the state variable equations of the system.

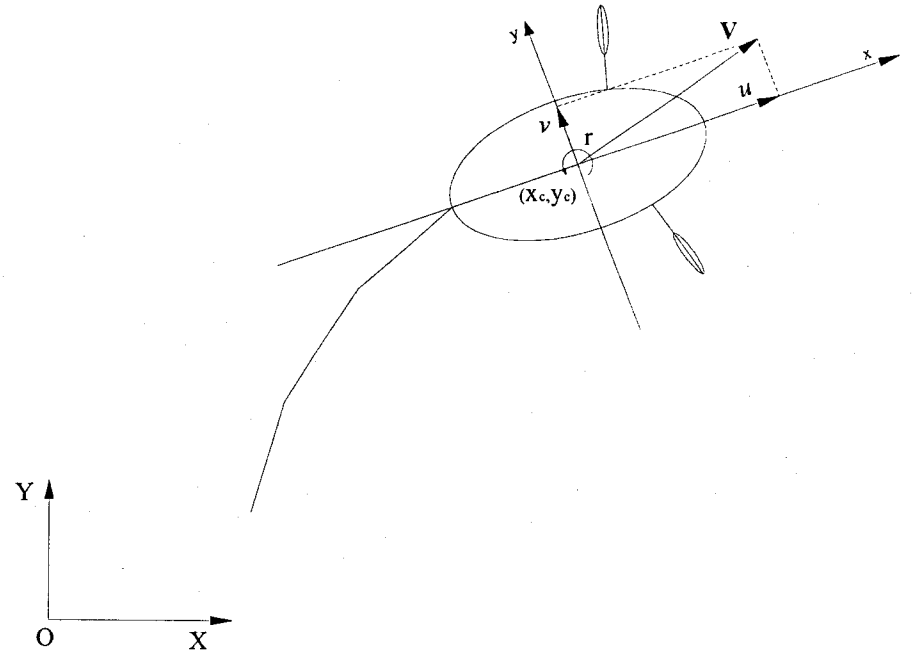

Fig. 18. Coordinate systems for the robotic fish model.

4.4 Parameter Identification

The parameters of the dynamic model (8-10) can be grouped together in the following manner in order to reduce the number of parameters that need to be identified

$$\dot{u} = P_1 vr - P_3 u + \tau_1 \tag{11}$$

$$\dot{v} = -P_1^{-1} ur - P_4 v \tag{12}$$

$$\dot{r} = P_2^{-1}(1 - P_1)uv - P_5 r + \tau_3 \tag{13}$$

where $P_1 = \frac{m_{22}}{m_{11}}$, $P_2 = \frac{m_{33}}{m_{11}}$, $P_3 = \frac{d_{11}}{m_{11}}$, $P_4 = \frac{d_{22}}{m_{22}}$, and $P_5 = \frac{d_{33}}{m_{33}}$. The normalized force and torque on the system are given by $\tau_1 = \frac{F_u}{m_{11}}$ and $\tau_3 = \frac{F_r}{m_{33}}$, respectively. These parameters are assumed to be a function of the oscillation frequency of the tail so that $\tau_1 = \tau_1(f)$ and $\tau_3 = \tau_3(f)$. For a given value of f they are constant so they can be identified as fixed parameters. These parameters can be found for different frequency values and a curve fit can be used to determine the normalized forces and torques as a function of frequency. Furthermore, it is assumed that a different set of parameters (and force/torque curve fits) can be identified for each mode of fish operation (forward and turning modes). When the fish changes modes of operation the parameters can be switched to the parameters for that particular mode. Alternatively, the parameters could be identified for different turning factors α and a lookup table could be formed. The amount of experimental data currently available was not extensive enough to form such a lookup table in this thesis work, so one set of parameters was determined for each mode of operation.

The local velocities *u, v,* and *r* and their derivatives were estimated from center finite difference approximations using the position and orientation measurements from the camera averaged over one cycle of the tail oscillation. A least squares curve fit for the derivatives of the local velocities in (11-13) was attempted in order to determine a set of parameters that minimized the approximation error. However, the parameters

obtained were not accurate due to excessive noise and model uncertainty in the experimental data. As such, the estimated parameters did not result in simulations that even captured the qualitative behaviour of the fish robot. In order to make the system identification procedure more tractable while still capturing the main qualitative behaviour of the fish motion, it was assumed that the transverse velocity v was approximately equal to zero. This approximation was motivated by the fact that the viscous friction in the transverse direction is much higher than the forward direction due to its much larger cross sectional area in that direction. The experimental data also supported this assumption. With this key assumption the equations of motion simplify to the following

$$T_1\dot{u} + u = T_1\tau_1 \tag{14}$$

$$T_3\dot{r} + r = T_3\tau_3 \tag{15}$$

where the time constants for the forward and rotational directions are given by $T_1 = \frac{1}{P_3}$ and $T_3 = \frac{1}{P_5}$, respectively. Therefore, the number of parameters that need to be identified is substantially reduced and their relation to the basic dynamic characteristics is more intuitive than before. Furthermore, the parameters can now be easily found by minimizing the error between the model solution (exponential functions with time constants of T_1 and T_3) and the experimentally measured forward and rotational velocities, u and r. This procedure is more robust than the previously mentioned least

squares curve fitting approach with its larger set of parameters determined from the more noisy derivatives of u and r. Therefore, it is less sensitive to noise and model uncertainty than the previous approach. Using the simplified identification procedure the following sets of parameters were found for the forward and turning modes. Note that for the case $\alpha = 0$ (forward motion) the parameters T_3 and τ_3 were given ideal default values since no significant rotational motion was observed.

f (Hz)	T_1 (s)	τ_1 (m/s^2)	T_3 (s)	τ_3 (rad/s^2)
1.0	0.7	0.1440	1	0
1.25	0.75	0.1651	1	0
2.0	0.85	0.1835	1	0

Table 3. Identified parameters for forward operation mode ($\alpha = 0$).

f (Hz)	T_1 (s)	τ_1 (m/s^2)	T_3 (s)	τ_3 (rad/s^2)
1.0	0.5	0.1337	0.7	0.2414
2.0	1.1	0.1529	0.92	0.3189

Table 4. Identified parameters for turning operation mode ($\alpha = 1$).

A comparison of the simulation of the identified models to the experimental data is

shown in Fig. 19 to Fig. 25. It is evident that the parameters result in approximations that capture the overall time constants of the system and the steady state values of the local velocities. The overall approximation provides good qualitative agreement with the experimental data, considering how much noise and model uncertainty is present in the experimental data.

Curve fits for the normalized force and torque as a function of the input frequency where performed using the parameter estimates for multiple frequencies. The second order polynomial equations used for the curve fits have the following form

$$\tau_1 = \sum_{i=0}^{2} a_i f^i \tag{16}$$

$$\tau_3 = \sum_{i=0}^{2} b_i f^i \tag{17}$$

where a_i and b_i are curve fitting parameters. The results of the curve fits are shown in the following tables for each mode of operation.

parameter	value	parameter	value
a_0	-0.0191	b_0	-0.0325
a_1	0	b_1	0.000
a_2	0.1528	b_2	0.2739

Table 5. Curve fit parameters for turning operation mode ($\alpha = 1$).

parameter	value	parameter	value
a_0	-0.0120	b_0	0
a_1	0.0092	b_1	0
a_2	0.1513	b_2	0

Table 6. Curve fit parameters for forward operation mode ($\alpha = 0$).

Comparisons of the curve fits to experimental data are shown in Fig. 26 to Fig. 28. It can be seen that the identified functions are definitely nonlinear with decreasing actuator effectiveness if the input frequency becomes too high. This phenomena was

frequently observed in the experiments. It is thought to be caused by bandwidth limitations of the servo motors and the swimming mechanism. However, it is also possible that the swimming motion becomes less efficient for higher frequencies. A detailed investigation with more advanced sensors is required to determine the exact cause of this behaviour. Actuator nonlinearity definitely appears to be a significant problem in modelling and control of this class of fish robots. Additional experiments and modelling research should be performed to more fully understand this problem and its implication for tail link trajectory optimization and control design.

Additional experimental data is required to perform a formal validation process of the model. This is the subject of planned future investigations. However, plots of the transverse velocity v for the model identification test conditions is illustrated in Fig. 29 and Fig. 30 for the case where the turning factor $\alpha = 1$. It should be noted that no significant transverse velocity was found for $\alpha = 0$. It can be seen that the magnitude of the transverse velocity v is small relative to the magnitude of the forward velocity u which supports one of the key assumptions made in the simplified identification process.

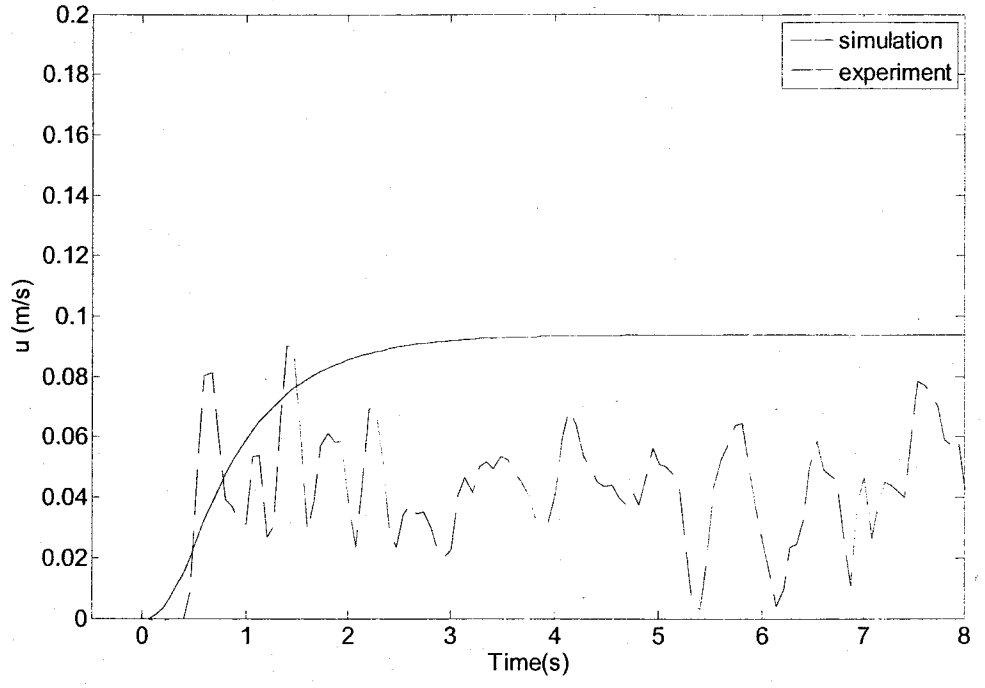

Fig. 19. Forward velocity versus time for $\alpha = 1$ and $f = 1$ Hz.

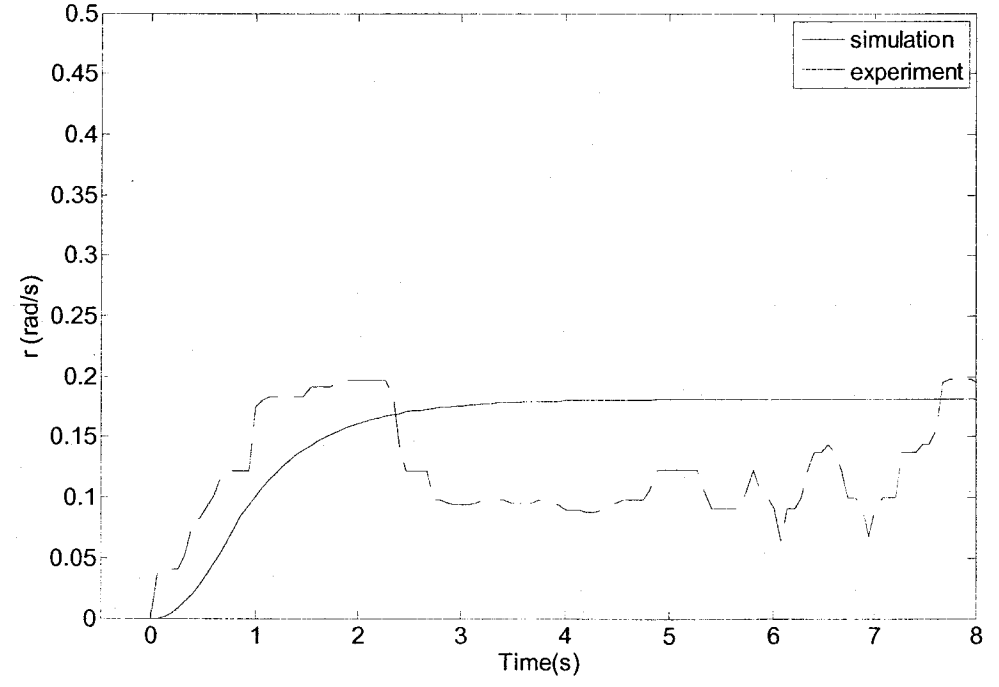

Fig. 20. Rotational velocity versus time for $\alpha = 1$ and $f = 1$ Hz.

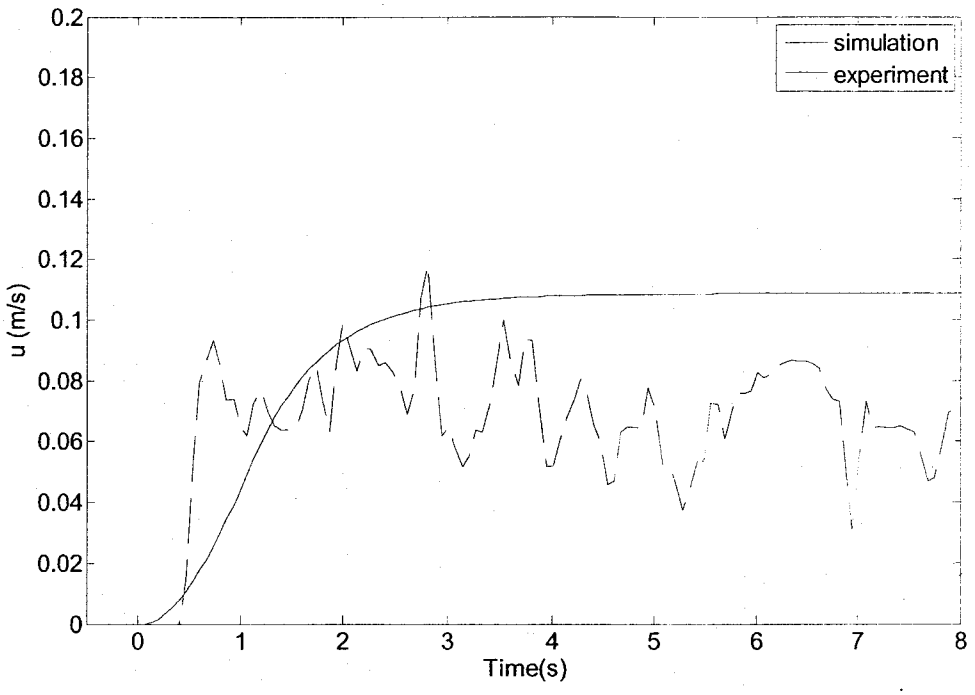

Fig. 21. Forward velocity versus time for $\alpha = 1$ and $f = 2$ Hz.

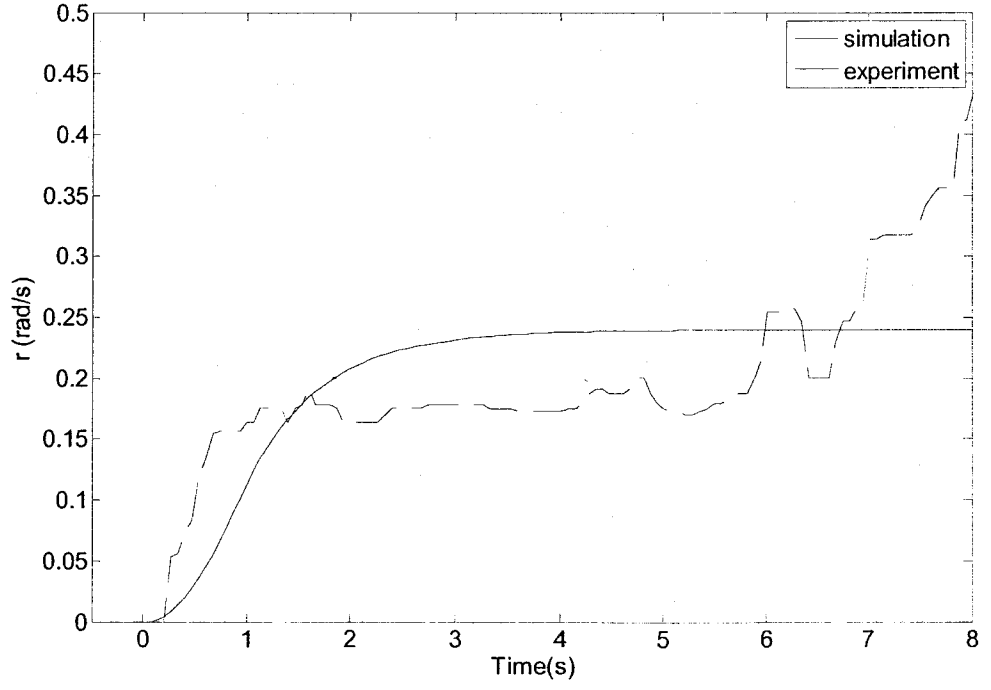

Fig. 22. Rotational velocity versus time for $\alpha = 1$ and $f = 2$ Hz.

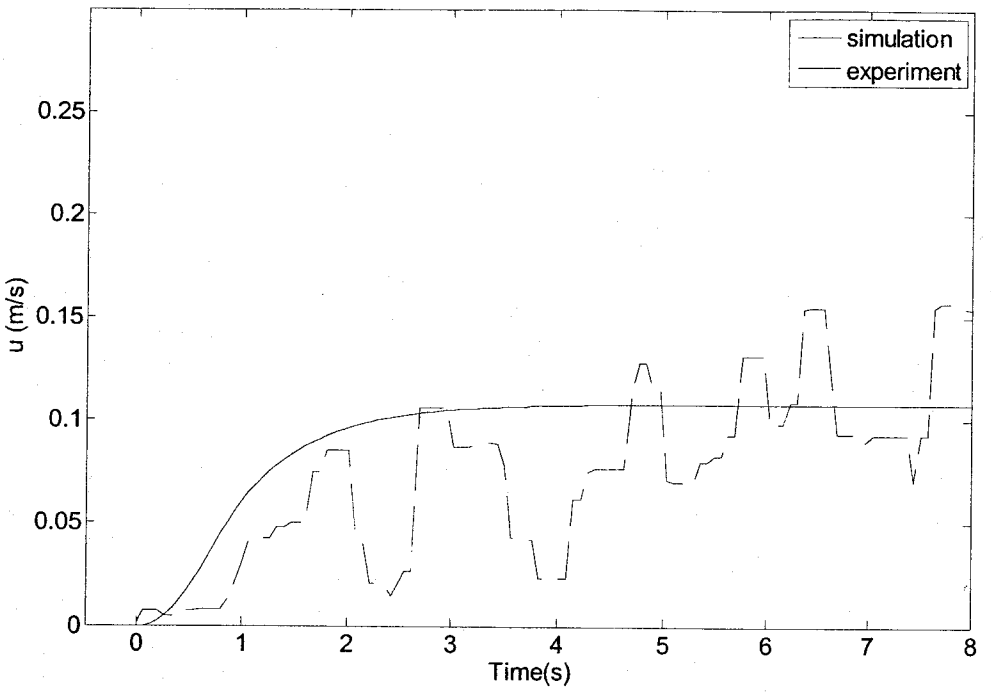

Fig. 23. Forward velocity versus time for $\alpha = 0$ and $f = 1$ Hz.

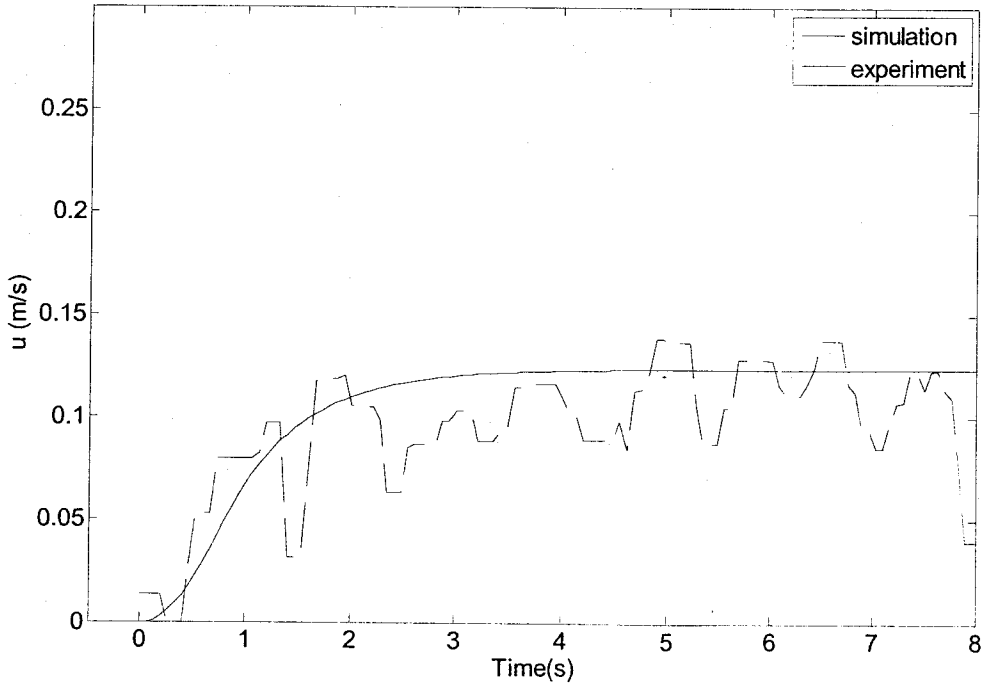

Fig. 24. Forward velocity versus time for $\alpha = 0$ and $f = 1.25$ Hz.

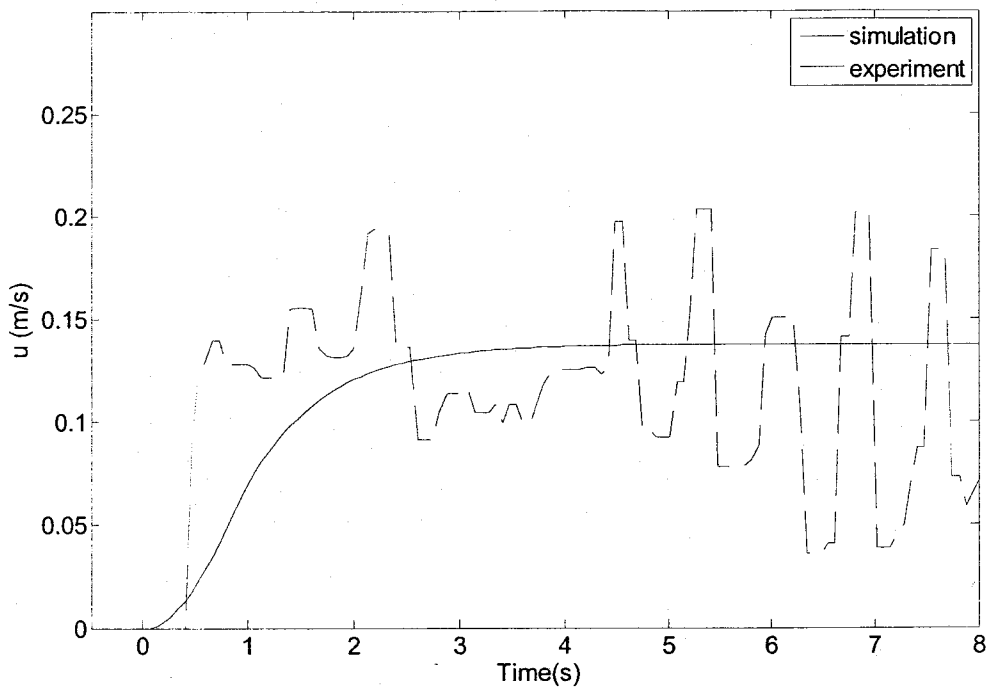

Fig. 25. Forward velocity versus time for $\alpha = 0$ and $f = 2$ Hz.

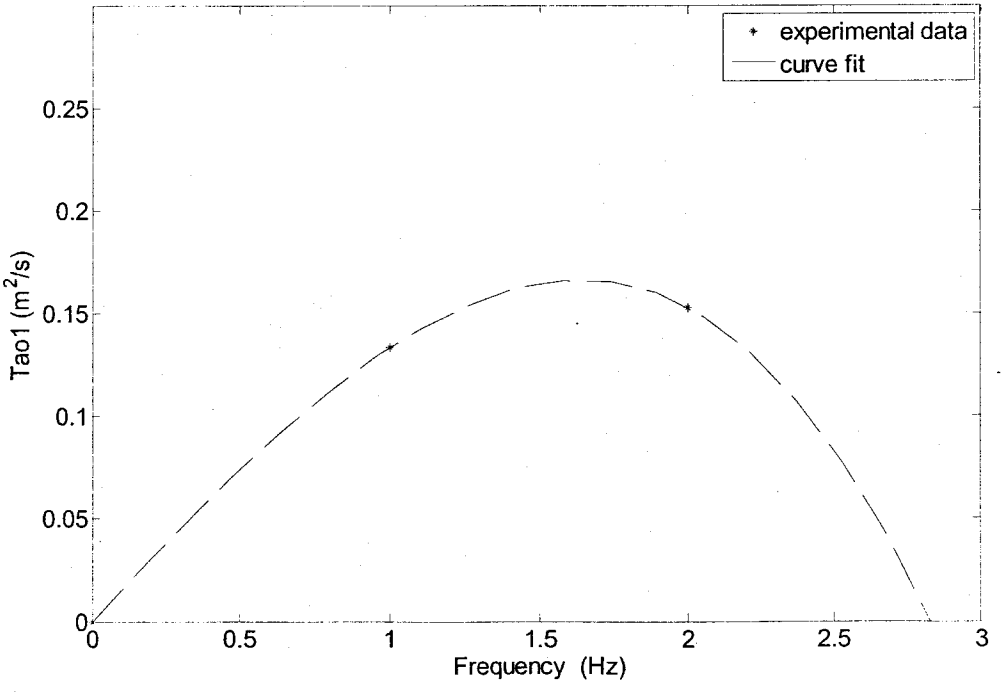

Fig. 26. Normalized force τ_1 versus frequency for $\alpha = 1$.

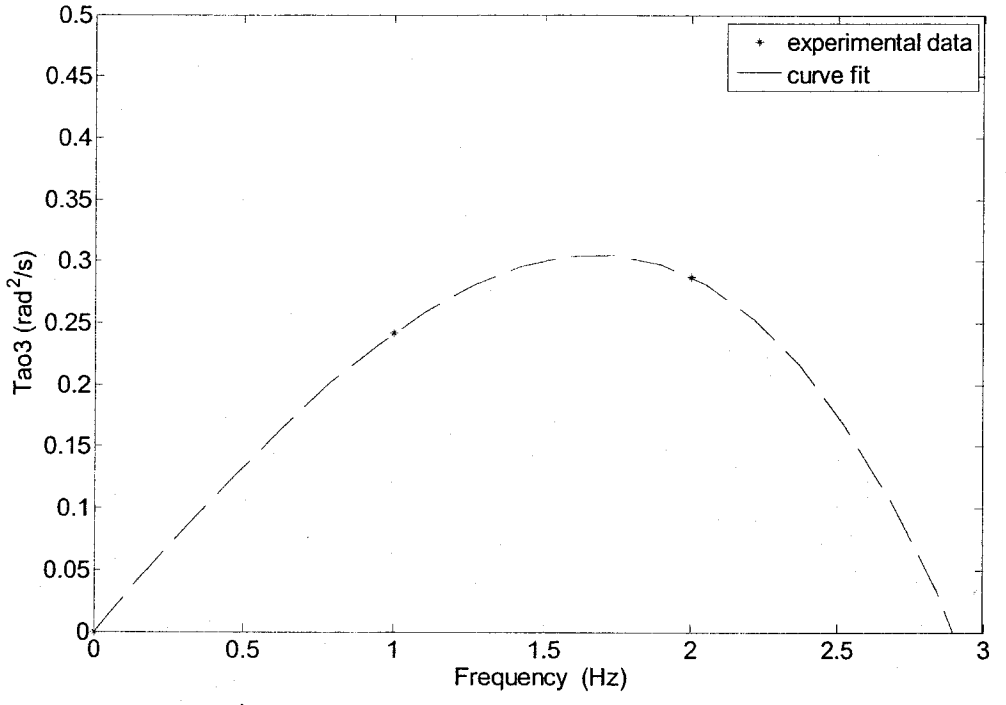

Fig. 27. Normalized torque τ_3 versus frequency for $\alpha = 1$.

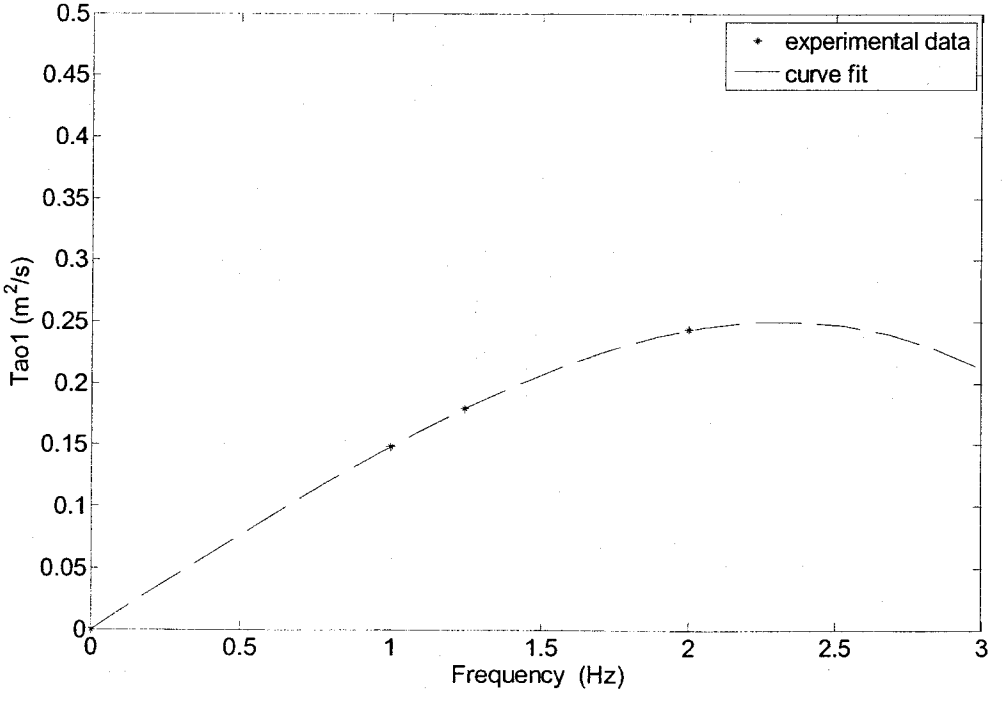

Fig. 28. Normalized force τ_1 versus frequency for $\alpha = 0$.

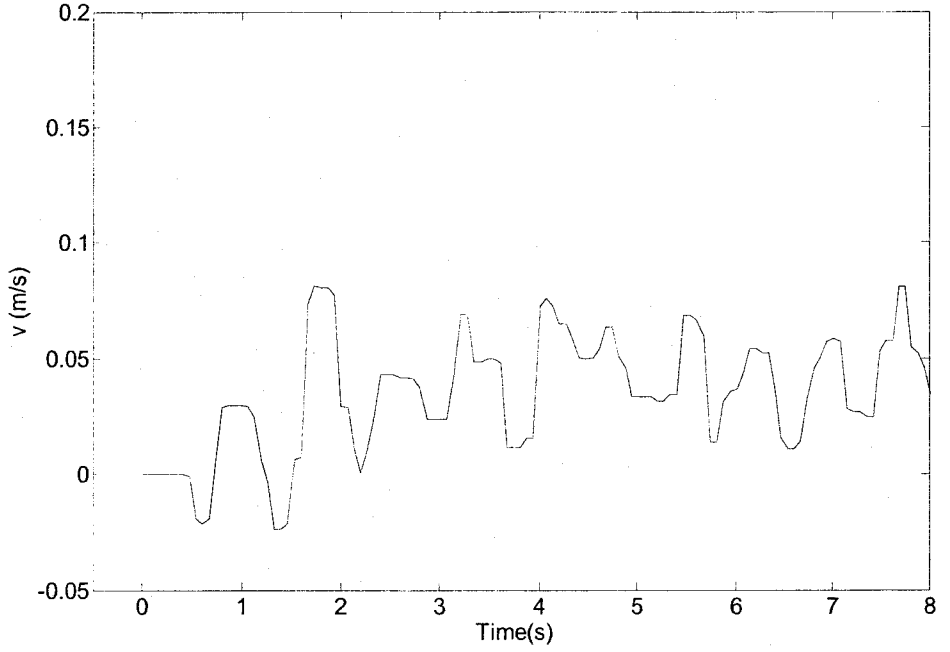

Fig. 29. Transverse velocity versus time for $\alpha = 1$ and $f = 1$ Hz.

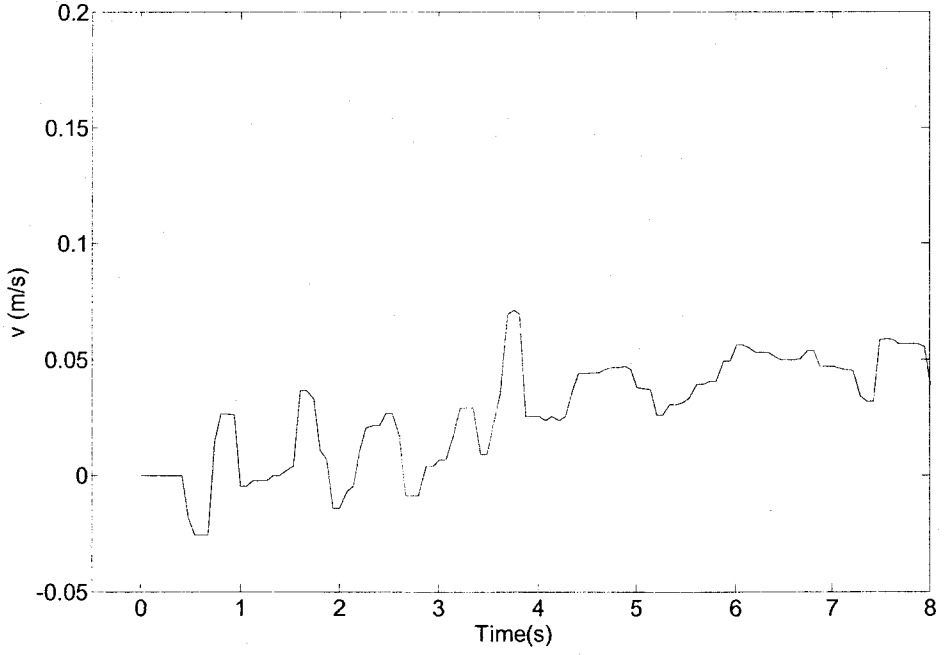

Fig. 30. Transverse velocity versus time for $\alpha = 1$ and $f = 2$ Hz.

4.5 MPF Actuation

In this section, a brief discussion of the MPF operating mode and the results of some related experimental tests are presented. To produce forward and turning motions using this mode of operation the following servo commands were used for the yaw angle $\psi(t)$ and pitch angle $\varphi(t)$ of the pectoral fins

$$\psi_l(t) = -k_l A_\psi \cos(2\pi ft) \tag{18}$$

$$\varphi_l(t) = A_\varphi \cos(2\pi ft + \frac{\pi}{2}) \tag{19}$$

$$\psi_r(t) = k_r A_\psi \cos(2\pi ft) \tag{20}$$

$$\varphi_r(t) = A_\varphi \cos(2\pi ft + \frac{\pi}{2}) \tag{21}$$

where A_ψ and A_φ are amplitude parameters for yaw and pitch, respectively. These parameters were optimized experimentally to obtain efficient motion. The variables k_l and k_r are control parameters. Setting k_l=1 and k_r=1 produces forward motion, whereas setting k_l=-1 and k_r=-1 produces backward motion. If k_l=1 and k_r=-1 the robotic fish turns right and if k_l=-1 and k_r=1 the fish turns left. The motivation for this choice of servo trajectories was based on the intuitive understanding of pectoral swimming motion obtained from [27],[29]. More research is required in order to determine optimal motion of the pectoral servomotors.

A dynamic model was not proposed for the MPF mode since the motion observed was small and intermittent due to the small capacity servos used in the current design. Therefore, the MPF motion violates the steady actuation assumption made in the proposed BCF model. As such, the proposed BCF modelling approach could not be applied. Development of a more complex dynamic model for MPF motion with unsteady actuation is left as a subject for future investigations. However, testing of the MPF mode did indicate some significant advantages over BCF actuation. It was found that the fish could consistently move both forward, backward, and rotate at small velocities with intermittent motion. The BCF actuation mode is not as consistent at small velocities and it cannot achieve backward motion. It is also difficult to achieve intermittent motion due to the steady nature of the tail actuation.

Illustration of the experimentally obtained MPF motion for forward, backward, and turning modes is shown in Fig. 31 to Fig. 37. This type of small intermittent motion could be useful in regulation control and for fine positioning control methods in cases when the robot fish gets close to its desired position. For instance, it can be seen that the direction of the fish during MPF oscillation (see Fig. 32) does not oscillate as it does during BCF motion (see Fig. 33) due to the reaction forces during an oscillation cycle of the tail. Another advantage of the MPF mode is that a smaller turning radius can be achieved than BCF mode. Fig. 38 compares the experimentally observed radius of curvature for both the BCF and MPF swimming modes. It can be seen that the fish robot has a much smaller turning radius in MPF mode. This is because not very much forward velocity is required to turn since the turning forces are mostly from the MPF fins. For the BCF mode significant forward velocity is required because a significant part of

the turning forces arise from the body movement through the water. From this experimental investigation, it can be seen that the MPF mode is a very promising approach that warrants more investigation from the standpoints of machine design, modelling, and control system development.

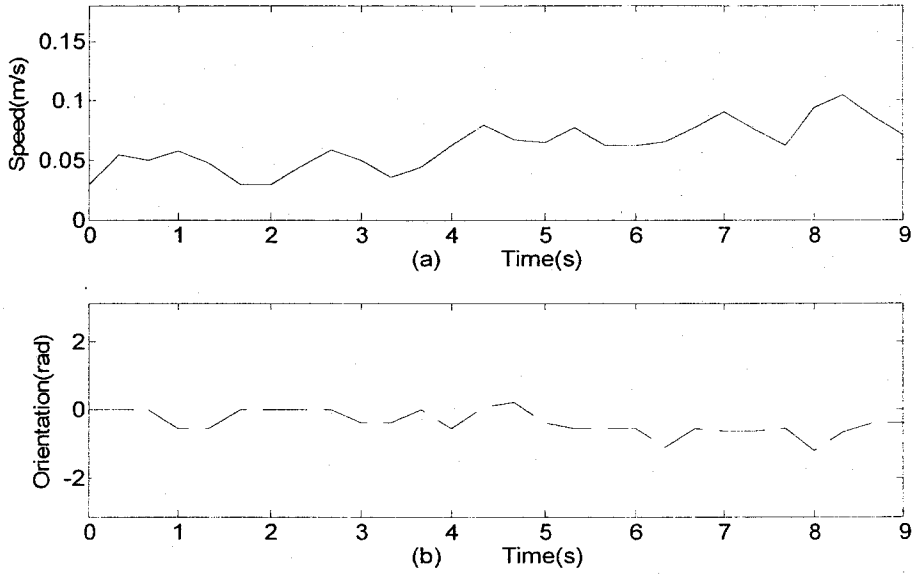

Fig. 31. Forward speed and orientation for forward MPF motion with *f=2* Hz.

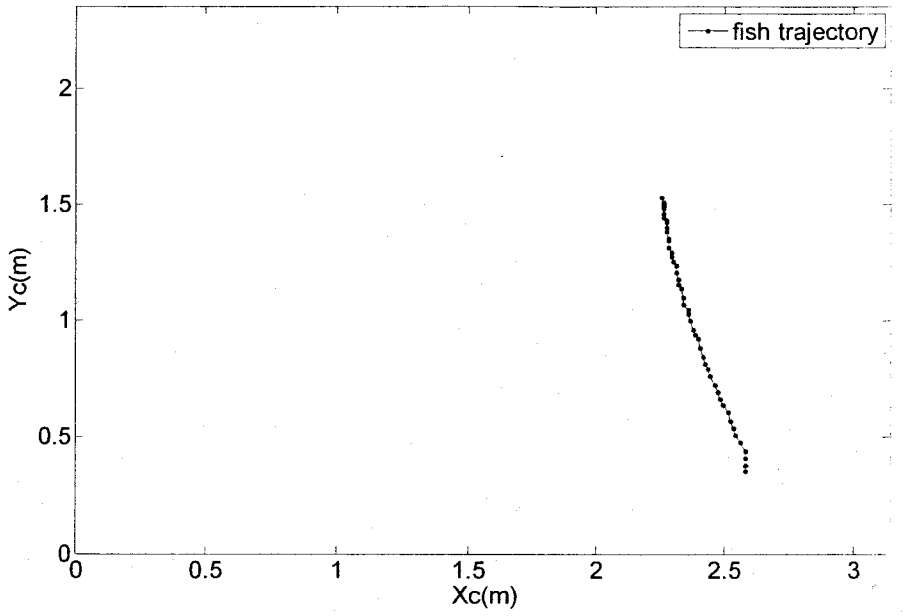

Fig. 32. Trajectory for forward MPF motion with *f=2* Hz.

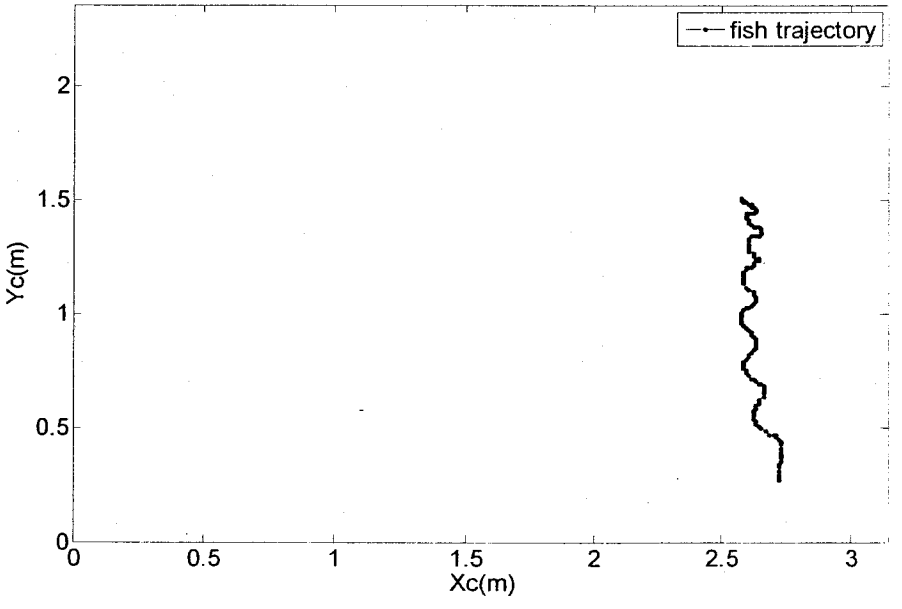

Fig. 33. Trajectory for forward BCF motion with *f=1* Hz.

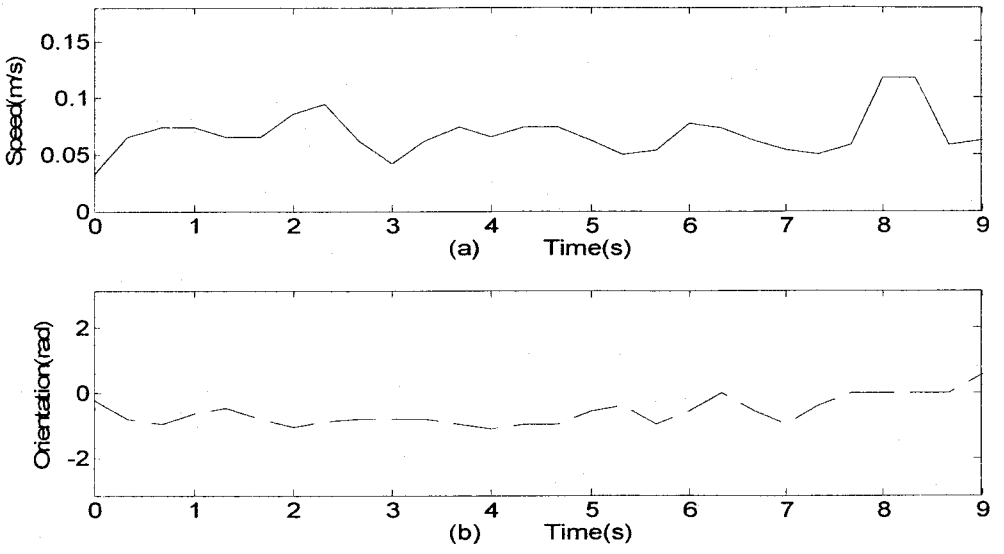

Fig. 34. Backward speed and orientation for backward MPF motion with *f=2* Hz.

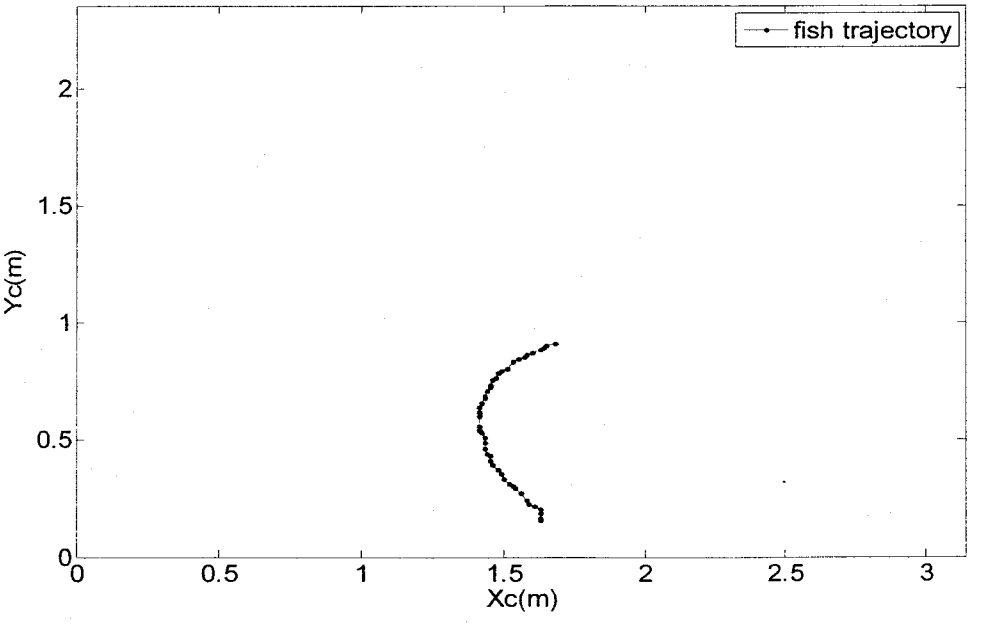

Fig. 35. Trajectory for backward MPF motion with *f=2* Hz.

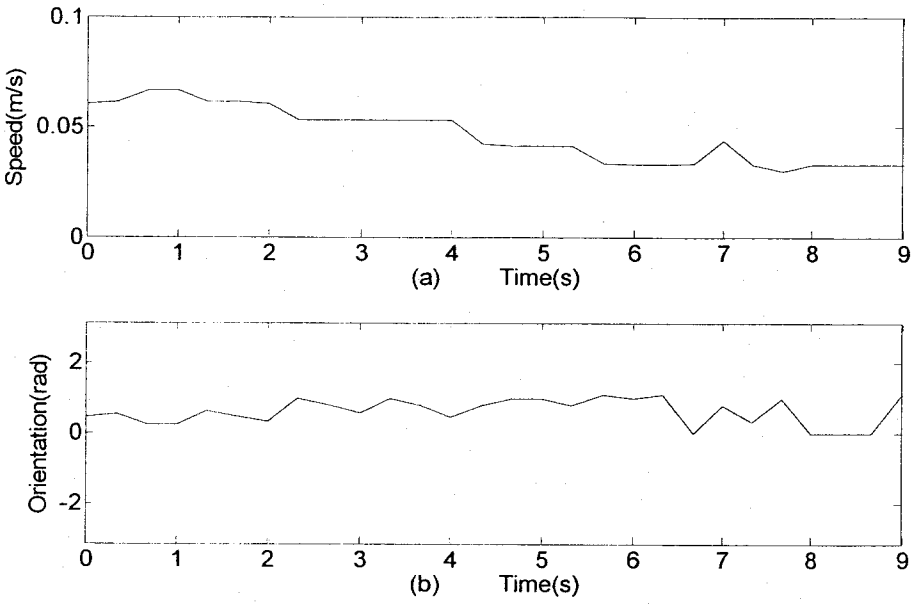

Fig. 36. Forward speed and orientation for right turning MPF motion with *f=1* Hz.

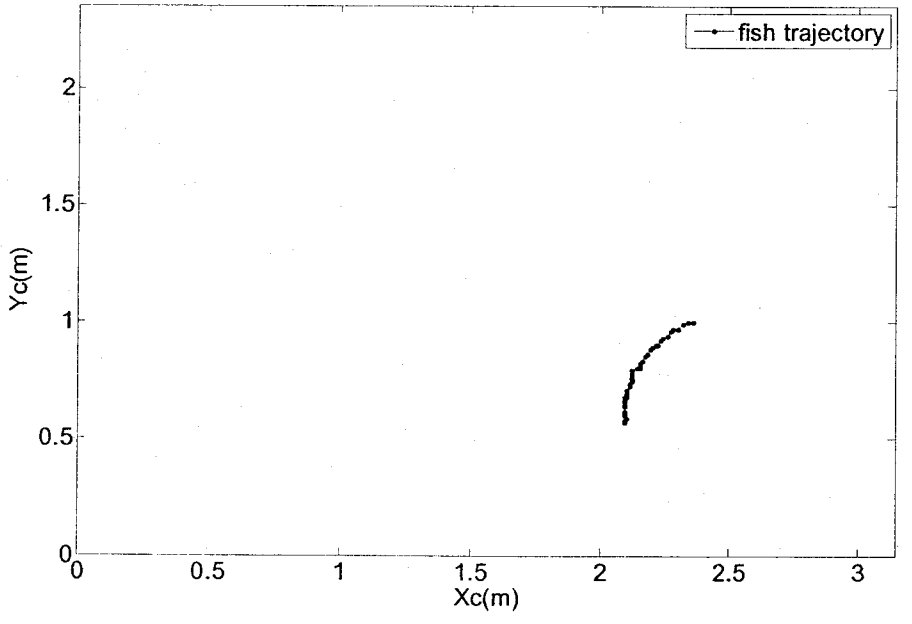

Fig. 37. Trajectory for right turning MPF motion with *f=1* Hz.

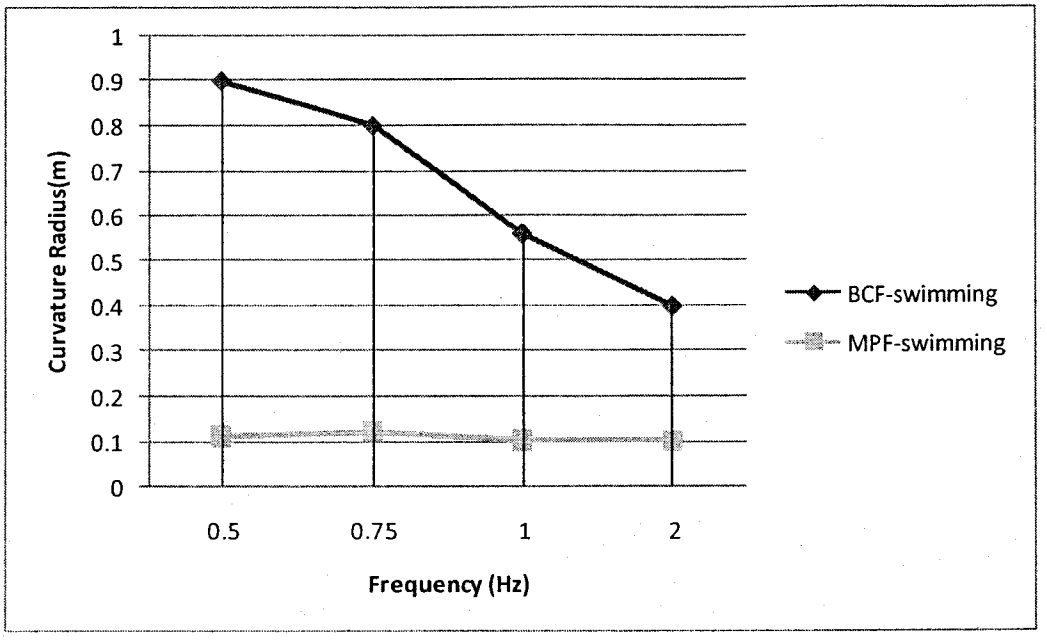

Fig. 38. Radius of curvature for BCF and MPF motion versus frequency.

5. Next Generation Robotic Fish

In this chapter, based on observations made during the experiments, improvement of the robotic fish design is discussed and a next generation design is proposed.

5.1 Areas for Improvement

During the implementation and testing process of the first generation robotic fish the following key areas for improvement were found.

1) The overall speed and agility could be increased including a smaller turning radius for BCF motion.

2) The swimming linkage mechanism could be improved in strength so that faster swimming frequencies and larger amplitudes can be employed, provided the servo motors are powerful enough.

3) The hinges employed in the linkage mechanism were joined by pins. Bearings were not used in the prototype due to limited machining resources available. However, bearings and high tolerance machined pieces would achieve significantly less friction, higher strength, and more swimming efficiency.

4) The robotic fish is too long to effectively turn in small swimming pool environments typically used in research labs.

5) The body and tail surface are not an ideal torpedo like streamlined shape. Therefore, the drag is relatively large making it harder to achieve high forward

speeds. Furthermore, the fish skin was constructed using a simple rubber balloon resulting in relatively high surface friction.

6) The body servo motors used have relatively limited power, torque, oscillation frequency, and rotational velocity specifications. This tends to limit the oscillation frequency of the tail and fins for a given amplitude.

7) The battery used was a 4.6V NiMH rechargeable model. The robotic fish could only swim for 30 minutes with this type of battery pack. A higher capacity battery pack could extend the swimming time of the robotic fish considerably.

8) A larger number of joints would more closely replicate the natural motion of a real fish. However, there is a trade-off with mechanical and controller complexity required for a larger number of joints.

5.2 Proposed New Design

A new design was developed based on the key areas for improvement listed in the previous section. The detailed drawings for this design are shown in Fig. 39 and the conceptual drawing is shown in Fig. 40. The overall dimensions of this robotic fish will be 0.4 m x 0.2 m x 0.1 m. The main components of the design will consist of high-torque servo motors, a gear box, pulleys, pectoral fins, and a tail fin. The frame of the robotic fish is made of aluminum and plastic. The skin is made from low friction rubber that is flexible, smooth, and waterproof. This new design has the following features and advantages.

1) Instead of three servomotors which are used in current robotic fish tail for

propulsion, the tail actuator of the new robotic fish will employ a single high torque servo motor for propulsion. A lower torque servo motor will be used to control the tail direction. This design will allow faster tail oscillations and swimming speeds since a more powerful servo motor could be employed than before. Some tail motion flexibility will be lost due to the reduction of the number of servos. However, it is assumed that the linkage and gear parameters will be selected to obtain near optimal swimming motion for the nominal operating conditions. This should be sufficient for many types of control research.

2) A gearbox will be employed for the high torque tail servo motor to increase the torque capacity and provide the ability to change the amplitude of the links by changing the gear ratio. The torque will be transmitted to each link by driving belts and pulleys. This sturdy mechanism will support the additional stresses associated with faster tail oscillations and higher swimming speeds. It will also result in less friction and more energy efficiency.

3) The new design is more compact due the use of a single high torque servo motor for the tail propulsion and the employment of stronger more compact linkages. The packaging of the pectoral fins was also improved. The new robotic fish will only be 0.4m long which will support a significantly smaller turning radius.

4) More powerful pectoral fins and servo motors will be employed to allow more significant moving capability in MPF mode.

5) A new material called Room Temperature Vulcanizing (RTV) rubber will be used to make the skin of the robotic fish. This material is waterproof and flexible with very low surface friction.

6) Real fish have the advantage of being able to sense where vortexes are located along their body. In the new fish design pressure sensors will be attached to each side of the tail in order too emulate this capability. This will allow more efficient actuation and more complex unsteady models to be developed and tested.

The features of the new proposed design will result in a robotic fish that is significantly better suited for modelling and control studies than the current prototype.

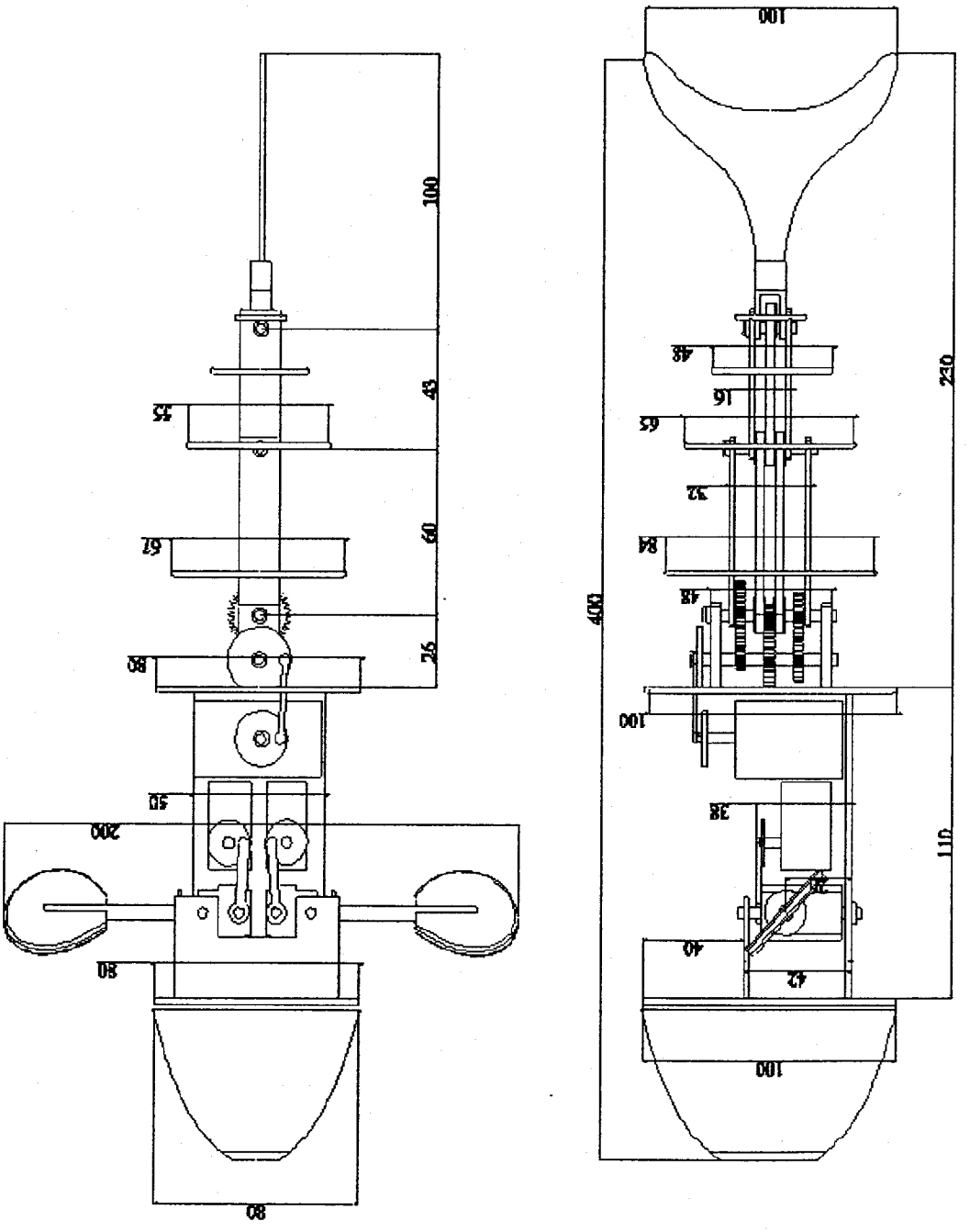

Fig. 39. Detailed drawings of the next generation robotic fish.

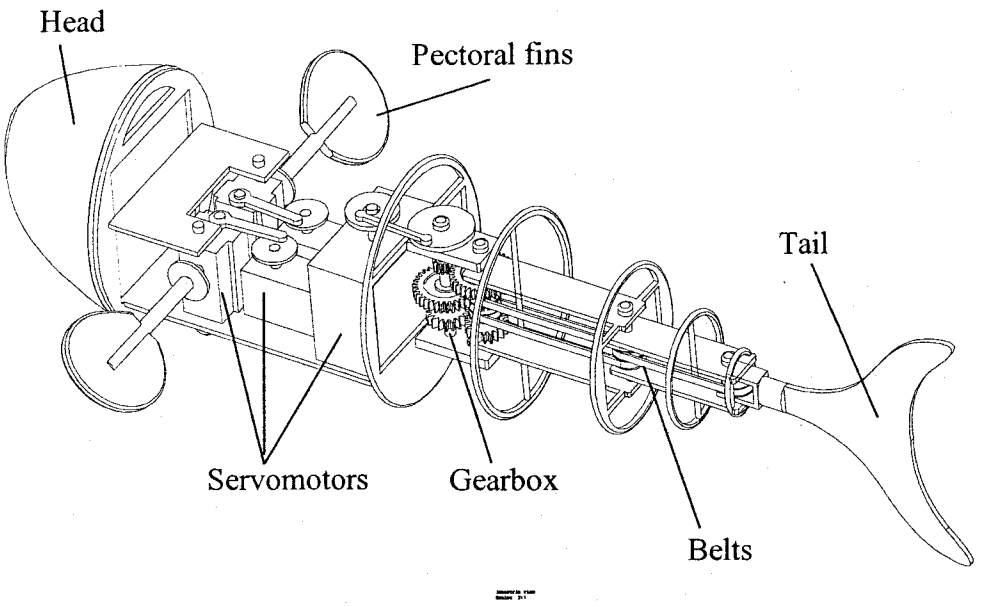

Fig. 40. Conceptual drawing of the next generation robotic fish.

6. Conclusions and Future Work

In this thesis, a novel robotic fish was designed and implemented. Experimental testing was performed and a relatively simple low order dynamic model was developed. The main contributions of the thesis are listed below.

1) A novel low cost robotic fish with both BCF actuation and MPF actuation was developed using radio controlled servos for actuation of the tail linkage and pectoral fins. The prototype is one of the first robotic fish to include both BCF and MPF actuation mechanisms.

2) The robotic fish was tested in a 10 m x 5 m x 1.8 m swimming pool environment demonstrating proof of concept and providing data for performance analysis and dynamic modelling.

3) A relatively simple low order dynamic model was developed assuming the fish can be modelled as a marine vessel with steady actuation. The key parameters were identified assuming the transverse velocity is negligible. Comparison to experimental data indicates the model captures the steady state velocity and time constants for the forward and turning modes of operation.

4) Based on experimental observations of the constructed prototype, a new generation fish design was proposed to provide faster swimming, higher energy efficiency, a smaller turning radius, and other significant improvements.

Together, these results provide a significant and novel experimental framework for future studies related to modeling and control of robotic fish systems. Future work

includes implementing and testing the improved robot design described in Chapter 5 and developing new dynamic models with unsteady actuation capable of modelling the MPF swimming mode. New control algorithms for robotic fish can also be developed and tested using the experimental framework developed.

References

[1] R. D. Beer, H . J. Cheil , R. D. Quinn, and et al, "Biorobotic approaches to the study of motor systems", *Current Opinion in Neurobiology*, vol.7, pp.777-782 , 1998.

[2] M. Sfakiotakis, D.M. Lane, and J. B. C. Davies. "Review of fish swimming modes for aquatic locomotion", *IEEE Journal on Oceanic Engineering*, vol.24, pp. 237-252, Apr. 1999.

[3] B. G. Tong, "Propulsive Mechanism of Fish's Undulatory Motion," *Mechanic in Engineering*, vol.22. No.3, pp. 69-74, 2000.

[4] J. M. Anderson, P. A. Kerrebrock, "The Vorticity Control Unmanned Undersea Vehicles (VCUUV) An Autonomous Vehicle employing fish swimming propulsion and manoeuvring", *Proc. Of 10th Int. Symp. on Unmanned Untethered Submersible Technology*, pp 189–195, 1997.

[5] M. S. Triantafyllou and G. S. Triantafyllou, "An efficient swimming machine", *Scientific American*, vol. 272, pp. 64–70, Mar. 1995.

[6] J. Yu, M. Tan, S. Wang, and E. Chen, "Development of a Biomimetic Robotic Fish and Its Control Algorithm", *IEEE Trans. Sys. Man and Cyber*, Part B, vol. 34, no. 4, pp. 1798–1810, 2003.

[7] C.C. Lindsey, "Form, function and locomotory habits", *Fish Physiology Vol. VII Locomotion, New York, Academic Press,* Vol.7, pp. 1-100,1978.

[8] J.J. Magnuson, " Locomotion by scombrid fishes: hydromechanics, morphology and behavior", *Fish Physiology Vol. VII Locomotion, New York: Academic Press*,Vol.7, pp. 239-313, 1978.

[9] S. Vogel, "Life in moving fluids", *Princeton: Princeton University Press*, 1994.

[10] T.L. Daniel, "Unsteady aspects of aquatic locomotion", *Integrative and Comparative Biology*, vol. 24, pp. 121-134, 1984.

[11] C.M. Breder, "The locomotion of fishes", *Zoologica*, vol. 4, pp. 159-256, 1926.

[12] J. Jalbert, S. Kashin, J. Ayers, "A biologically-based undulatory lamprey-like AUV", *Proceeding of the Autonomous Vehicles in Mine Countermeasures Symposium, Naval Postgraduate School*, pp. 39-52, 1995.

[13] S. Guo, T. Fukuda, N. Kato, K. Oguro, "Development of Underwater Micro-robot Using ICPF Actuator", *Proc. of IEEE Int. Conference on Robotics and Automation, Leuven, Belgium*, pp. 1829-1834, 1998.

[14] N. Kato, "Control performance in the horizontal plane of a fish robot with mechanical pectoral fins", *IEEE Journal of Oceanic Engineering*, 25(1), pp. 121-129, 2000.

[15] K.A. Morgansen,Vincent Duindam,Richard J. Mason."Nonlinear Control Methods for Planar Carangiform Robot Fish Locomotion". *Proceeding of the 2001 IEEE International Conference on Robotics and Automation*. pp 427-434.

[16] J.J. Videler, "Fish Swimming". *London: Chapman & Hall*, 1993.

[17] P.W. Webb, "The biology of fish swimming," in *Mechanics and Physiology of Animal Swimming. Cambridge University Press.UK.*, pp. 45-62,1994.

[18] P.W. Webb, "Form and function in fish swimming", *Scientific American*, vol. 251, pp. 58-68, 1984.

[19] Dennis R. G. & Herr H., MIT Biomechatronics homepage http://www.ai.mit.edu/people/hherr/biomech.html

[20] Hirata,K,"Design and Manufacturing of a Small Fish Robot", *Processing of Japan Society for Design Engineering*, No 99.pp 29-32.

[21] Hirata.K,Warashina.S,"Study on Turning Performance of Experimental Fish Robot" *Processing of Japan Society for Design Engineering*, Tohoku Branch. pp 68-71.

[22] Ura.T, Takagawa.S, "Underwater Robots", Seizan-Do,1994.

[23] J. Liu, H. Hu and D. Gu," A layered control architecture for robotic fish", *Proc. of IEEE/RSJ Int. Conf. on Intelligent Robots & Systems*, Beijing, China, 9-15 Oct. 2006

[24] J.Z.Yu, E.K.Chen,S.Wang, M.Tan, "Research Evolution and Analysis of Biomimetic Robot Fish". *Control Theory and Application. Accepted in China*.2002

[25] R.W. Blake, "Undulatory median fin propulsion of two teleosts with different modes of life", *Canadian Journal of Zoology*, vol. 58, pp. 2116-2119, 1980.

[26] R.W. Blake, "Median and paired fin propulsion", in *Fish Biomechanics. New York: Praeger Publishers*, pp. 214-247. 1983.

[27] M.W. Westneat and J.A. Walker, "Applied aspects of mechanical design, behavior, and performance of pectoral fin swimming in fishes", in *Proc. of the Special Session on Bio- Engineering Research Related to Autonomous Underwater Vehicles, 10th Intern.*

Symp. Unmanned Untethered Submersible Technology, New Hampshire, USA, pp. 153-165, September 1997.

[28] A.C. Gibb, B.C. Jayne and G.V. Lauder, "Kinematics of pectoral fin locomotion in the bluegill sunfish", *Journal of Experimental Biology*, vol. 189, pp. 133-161, 1994.

[29] G.V. Lauder and B.C. Jayne, "Pectoral fin locomotion in fishes: testing drag-based models using 3-dimensional kinematics", *Integrative and Comparative Biolog,* vol. 36, pp. 567-581, 1996.

[30] C. Thorbole, B. Bahr, "Designing an Robotic Boxfish for the Mechatronics Course", *Icee2002*, 2002

[31] M.S.Triantafyllou,G.S.Triantafyllou,M.A.Grosenbauch,"Optimal thrust development in oscillating foil with application to fish propulsion", *Journal of Fluid and Structures*, Vol. 7,pp.205-224,1993.

[32] G. B. Gillis, "Undulatory locomotion in elongate aquatic vertebrates: Anguilliform swimming since Sir James Gray," *Amer. Zool.*, vol. 36,pp. 656–665, 1996.

[33] M. J. Lighthill, "Hydromechanics of aquatic animal propulsion", *Journal of Fluid and Structures.* vol. 1, pp. 413–466, 1969.

[34] R. W. Blake, "On ostraciiform locomotion," *Journal of Marine Biologic Assoc.*, vol.57, pp. 1047–1055, 1977.

[35] R. McN. Alexander, "Functional Design in Fishes", Hutchinson Univ. London, U.K, , Chapter 2 ,1967.

[36] P. W. Webb, "Is the high cost of body caudal fin undulatory swimming due to increased friction drag or inertial recoil?" *Journal of Exp. Biol.*, vol. 162, pp. 157–166, 1992.

[37] H. Liu, R. Wassersug, and K. Kawachi, "The three-dimensional hydrodynamics of tadpole locomotion," *Journal of Experimental Biology* ,vol. 200, pp. 2807–2819,1997.

[38] G. S. Triantafyllou, M. S. Triantafyllou, and M. A. Grosenbauch, "Optimal thrust development in oscillating foils with application to fish propulsion," *Journal of Fluid and Structures*, vol. 7, pp. 205–224, 1993.

[39] U. K. M¨uller, B. L. E. Van den Heuvel, E. J. Stamhuis, and J. J. Videler, "Fish foot prints: Morphology and energetics of the wake behind continuously swimming mullet", *Journal of Experimental Biology*, vol. 200, pp. 2893–2906, 1997.

[40] J. M. Anderson, K. Streitlien, D. S. Barrett, and M. S. Triantafyllou, "Oscillating foils of high propulsive efficiency," *Journal of Fluid Mechanics*, vol. 360, pp. 41–72, 1998.

[41] M. W. Rosen, "Water flow about a swimming fish," China Lake, CA, US Naval Ordnance Test Station TP 2298, p. 96, 1959.

[42] J. Gray, "Studies in animal locomotion. VI. The propulsive powers of the dolphin," *Journal of Experimental Biology* ,vol. 13, pp. 192–199, 1936.

[43] J. M. Anderson, "Vorticity control for efficient propulsion," Ph.D. dissertation, Massachusetts Inst. Technol./Woods Hole Oceanographic Inst. Joint Program, Woods Hole, MA, 1996.

[44] R. Gopalkrishnan, M. S. Triantafyllou, G. S. Triantafyllou, and D. Barrett, "Active vorticity control in a shear flow using a flapping foil," *Journal of Fluid Mechanics*, vol. 274, pp. 1–21, 1994.

[45] K. Streitlien, G. S. Triantafyllou, and M. S. Triantafyllou, "Efficient foil propulsion through vortex control," *The American Institute of Aeronautics and Astronautics Journal*, vol. 34, pp. 2315–2319,1996.

[46] D. Weihs, "Some hydromechanical aspects of fish schooling," in *Swimming and Flying in Nature*, vol. 2, pp. 703–718, 1975.

[47] G. Taylor, "Analysis of the swimming of long narrow animals," in *Proceedings of the Royal Society*, vol. 214, pp. 158–183, 1952.

[48] T. Y. Wu, "Swimming of a waving plate," *Journal of Fluid Mechanics*, vol. 10, pp. 321–344, 1961.

[49] M. J. Lighthill, "Note on the swimming of slender fish", *Journal of Fluid Mechanics* vol. 9, pp. 305–317, 1960.

[50] M. J. Lighthill , "Aquatic animal propulsion of high hydromechanical efficiency" ,*Journal of Fluid Mechanics* ,vol. 44, pp. 265–301, 1970.

[51] M. J. Lighthill, "Large-amplitude elongated-body theory of fish locomotion", *Proceedings of the Royal Society*, vol. 179, pp. 125–138, 1971.

[52] C. S. Wardle and A. Reid, "The application of large amplitude elongated body theory to measure swimming power in fish", *Fisheries Mathematics*, pp. 171–191, 1977.

[53] J. Y. Cheng and R. Blickhan, "Note on the calculation of propeller efficiency using elongated body theory," *Journal of Experimental Biology*, vol. 192, pp.169–177, 1994.

[54] J. Katz and D. Weihs, "Large amplitude unsteady motion of a flexible slender propulsor", *Journal of Fluid Mechanics* ,vol. 89, pp. 713–723, 1979.

[55] T. Kambe, "The dynamics of carangiform swimming motions," *Journal of Fluid Mechanics*, vol. 87, pp. 533–560, 1978.

[56] T. Y. Wu, "Hydrodynamics of swimming propulsion. Part 3. Swimming and optimum movement of slender fish with side fins," *Journal of Fluid Mechanics,*vol. 46, pp. 521–544, 1971.

[57] J. N. Newman and T. Y. Wu, "A generalized slender-body theory for fish-like forms," *Journal of Fluid Mechanics* ,vol. 57, pp. 673–693, 1973.

[58] J. N. Newman, "The force on a slender fish-like body," *Journal of Fluid Mechanics*,vol. 58, pp. 689–702, 1973.

[59] D. Weihs, "A hydromechanical analysis of fish turning manuevers," in *Proceedings of the Royal Society*, vol. 182, pp. 59–72, 1972.

[60] D. Weihs, "The mechanism of rapid starting of slender fish," *Biorheology*,vol. 10, pp. 343–350, 1973.

[61] B. G. Tong, L. X. Zhuang, and J. Y. Cheng, "The hydrodynamic analysis of fish propulsion performance and its morphological adaptation," in *Sadhana-Academy Proc. in Eng. Sciences*, vol. 18, pp. 719–728, 1993.

[62] R. G. Root and J. H. Long, Jr., "A virtual swimming fish: Modeling carangiform fish locomotion using elastic plate theory," in *Proc. Special Session on Bio-Engineering Research Related to Autonomous Underwater Vehicles, 10th Intern. Symp. Unmanned Untethered Submersible Technology*, NH, in addendum, Sept. 1997.

[63] R. W. Blake, "Mechanics of ostraciiform propulsion," *Canadian Journal of Zoology*, vol. 59, pp. 1067–1071, 1981.

[64] Farbod Fahimi, "Sliding-Mode Formation Control for Underactuated Surface Vessel," *IEEE Transactions on Robotics*, vol. 23, No 3, Jun 2007.

[65] J,YUH, "Modeling and Control of Underwater Robotic Vehicles," *IEEE Transactions on System, Man and Cybernetics*, vol. 20, No 6, Nov 1990.

[66] M.Caccia,G.Veruggio, "Guidance and Control of a Reconfigurable Unmanned Underwater Vehicle," *Control Engineering Practice*, vol.21-37 , 2000.